Supporting Information

Praseodymium-selenium connecting selenotungstate containing mixed building blocks for catalytic synthesis of aza-heterocycles

Guoping Yang,†[a] Jiawei Cao,†[a] Zhoufu Lin,[a] Shixiong Li,*[b] Yayu Dong,*[c] Yufeng Liu*[a]

[a]Jiangxi Key Laboratory for Mass Spectrometry and Instrumentation, Jiangxi Province Key Laboratory of Synthetic Chemistry, East China University of Technology, Nanchang 330013, China.

[b]School of Mechanical and Resource Engineering, Wuzhou University, Wuzhou, Guangxi 543003, P. R. China.

[c]School of Materials Science and Engineering, East China Jiaotong University, Nanchang, 330013, China.

*Corresponding Author: lsx1324@163.com (S. X. Li); zmyydong@163.com (Y. Y. Dong); yfliu@ecut.edu.cn (Y. F. Liu).

†These authors contributed equally to this work.

Table of Contents

1. General Information

Materials and Methods

The FT-IR spectrum was obtained by using a Fourier transform infrared (FT-IR) (4000-500 cm^{-1}) spectrometer (Thermo Nicolet iS5) at 0.5 cm^{-1} resolution and 16 scans. Inductively coupled plasma optical emission spectrum (ICP-OES) data were obtained on an Agilent 725 ICP-OES spectrometer. Powder X-ray diffraction (PXRD) was performed on a Bruker D8 Advance diffractometer with Cu Kα radiation (λ = 1.5406 Å) at room temperature. Flash column chromatography was performed using silica gel of 200-300 mesh. The GC analysis was performed on Agilent 7890B equipped with a capillary column (HP-5, 30 m × 0.25 μm) using a flame ionization detector. The GC-MS were recorded on Agilent 7890B-7000D and Thermo Fisher/ISQ7000.

X-ray Crystallography

The single crystal X-ray diffraction data were collected on Bruker D8 Smart Apex II diffractometer with graphite monochromated Mo Kα radiation (λ = 0.71073 Å). Intensities were collected by *ω*-scan and reduced on *APEX 3* and a multi-scan absorption correction was applied.[1] The structures were solved and refined on *Olex2* using *SHELX* package.[2] Parameters of the crystal data collection and refinement are given in Table S1. The CCDC number is 2373607.

2. Experimental

Synthesis of Bc-Pr

$Na_2WO_4 \cdot 2H_2O$ (1.9791 g, 6 mol), Na_2SeO_3 (0.1383 g, 0.8 mmol), NH_4Cl (0.3209 g, 6 mmol), DL-malic acid (0.0402 g, 0.3 mmol) was dissolved in 20 mL deionized water and stirred for 30 min. The pH value of the solution was adjusted to 4.5 by 6 M HCl. Then $PrCl_3 \cdot 6H_2O$ (0.2133 g, 0.6 mmol) was added, and the final pH of the solution was adjusted to 3.5 by 1 M HCl and stirred for 30 min. Ultimately, the solution was filtered. About five weeks later, light green block crystals were obtained through evaporation (yield: 36% based on W). Anal. cal. (found %) for: $C_4H_3Na_{2.5}O_{118.5}Pr_{2.5}Se_{4.25}W_{30}$: C 2.24, H 1.28, N 0.87, W 59.93, Dy 5.05, Sb 3.78, Na 2.14, O 24.34.

Typical procedure of the condensation reaction

In a reaction vial of 4 mL, 2-aminobenzamide (**1**, 0.2 mmol), aldehyde (**2**, 0.2 mmol), **BC-Pr** (0.6 mol%) and EtOH (1 mL) were added. Then the reactions were carried out in screw cap vials with a Teflon seal at 100 °C for 1.5 h. After cooling to room temperature, the mixture was further purified by column chromatography (petroleum ether/EtOAc) to afford the desired products.

3. Characterization

Table S1. Crystallographic data and structure refinement of **BC-Pr** (SQUEEZE).

Code	**BC-Pr**
CCDC	2373607
Empirical formula	$C_4H_3Na_{2.5}O_{118.5}Pr_{2.5}Se_{4.25}W_{30}$
Fw	8207.89
T (K)	150
Crystal system	monoclinic
Space group	*C2/c*
a (Å)	64.919(4)
b (Å)	17.6777(10)
c (Å)	32.1895(19)
α (°)	90
β (°)	117.918(2)
γ (°)	90
V /Å^3	32642(3)
Z	8
ρ_{calcd} (g·cm^{-3})	3.340
μ (mm^{-1})	22.809
F (000)	28116.0
Crystal size (mm^3)	0.15 × 0.106 × 0.07
2 Θ range for data collection (°)	4.442 to 50
Index ranges	-77 ≤ h ≤ 77, -21 ≤ k ≤ 20, -38 ≤ l ≤ 38
Reflections collected	150226
Unique reflections	28706 (R_{int} = 0.0951)
Parameter	2305
Restraints	3243
GOOF on F^2	1.098
Final R indexes [I>=2σ (I)]	R_1 = 0.0582, wR_2 = 0.1406
Final R indexes [all data]	R_1 = 0.0831, wR_2 = 0.1488
Largest diff. peak/hole / e Å-3	1.97/-1.96

$^aR_1 = \sum||F_o|-|F_c||/\sum|F_o|$, $^bwR_2 = \{\sum[w(F_o^2-F_c^2)^2]/\sum[w(F_o^2)^2]\}^{1/2}$

Table S2. Bond valence calculations for Pr, W, Se, and selected O atoms in **BC-Pr**.

Atom	BVS	Valence	Atom	BVS	Valence
Pr1	3.03	+3	W15	6.25	+6
Pr2	3.37	+3	W16	6.03	+6
Pr3	3.29	+3	W17	6.40	+6
Se1	3.75	+4	W18	6.70	+6
Se2	3.82	+4	W19	6.55	+6
Se3	3.97	+4	W20	6.36	+6
Se4	4.06	+4	W21	5.99	+6
W1	5.72	+6	W22	5.99	+6
W2	5.95	+6	W23	6.32	+6
W3	6.23	+6	W24	6.01	+6
W4	5.98	+6	W25	6.08	+6
W5	5.97	+6	W26	6.32	+6
W6	5.88	+6	W27	6.35	+6
W7	5.32	+5	W28	5.83	+6
W8	7.28	+6	W29	5.96	+6
W9	6.15	+6	W30	6.28	+6
W10	6.34	+6	O1W	0.39	H_2O
W11	5.85	+6	O2W	0.32	H_2O
W12	5.91	+6	O3W	0.30	H_2O
W13	6.19	+6	O4W	0.36	H_2O
W14	5.74	+6	O106	1.49	O^{2-}

Bond valence sum (BVS) analysis: The BVS values (V*i*) of metal atoms were calculated using the following equation:[3]

$$V_i = \Sigma\exp[(r_0\text{-}r_{ij})/B] \qquad (1)$$

where r_0 is the bond valence parameter for a given atom pair, r_{ij} is the bond length between atoms *i* and *j* obtained from the crystal structure.

Table S3. Comparison of the present catalytic system with other reported catalysts in the synthesis of products **3a** (Entries 1-6) and **5a** (Entries 7-11)

Entry	Catalyst	Loading/mol%	Time/h	Solvent	T/°C	Yield / %	Ref.
1	**BC-Pr**	**0.6**	**1.5**	**EtOH**	**100**	**95**	**This work**
2	In-MOF	1	10	EtOH	reflux	99	4
3	Nd-MOF	10	24	CH_3CN	rt	99	5
4	$CoFe_2O_4$@Pr	50 mg	2	EtOH	reflux	92	6
5	Cu-MOF Nanosheet	5	12	MeOH	70	94	7
6	NiUMo	3	2	CH_3CN	90	93	8
7	**BC-Pr**	**0.6**	**1.5**	**EtOH**	**100**	**88**	**This work**
8	In-MOF	5	24	EtOH	reflux	84	5
9	CAN-SiO_2	5	0.15	Toluene	rt	94	9
10	Amberlyst-15	10	0.5	H_2O	ultrasound	92	10
11	$Sc(OTf)_3$ / Pybox	10 / 20	24	CH_2Cl_2	-40	66	11

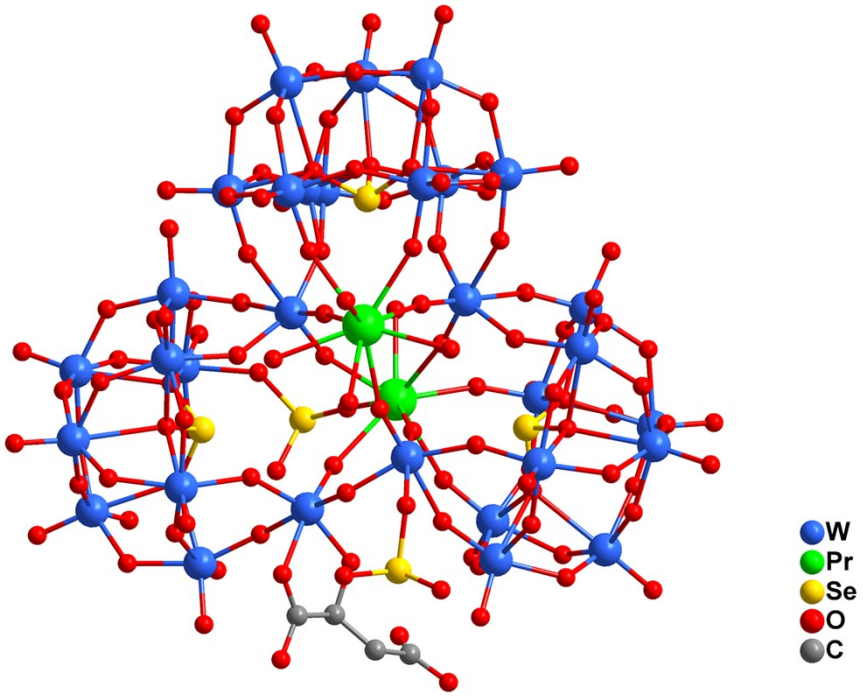

Figure S1. The structure of **BC-Pr**.

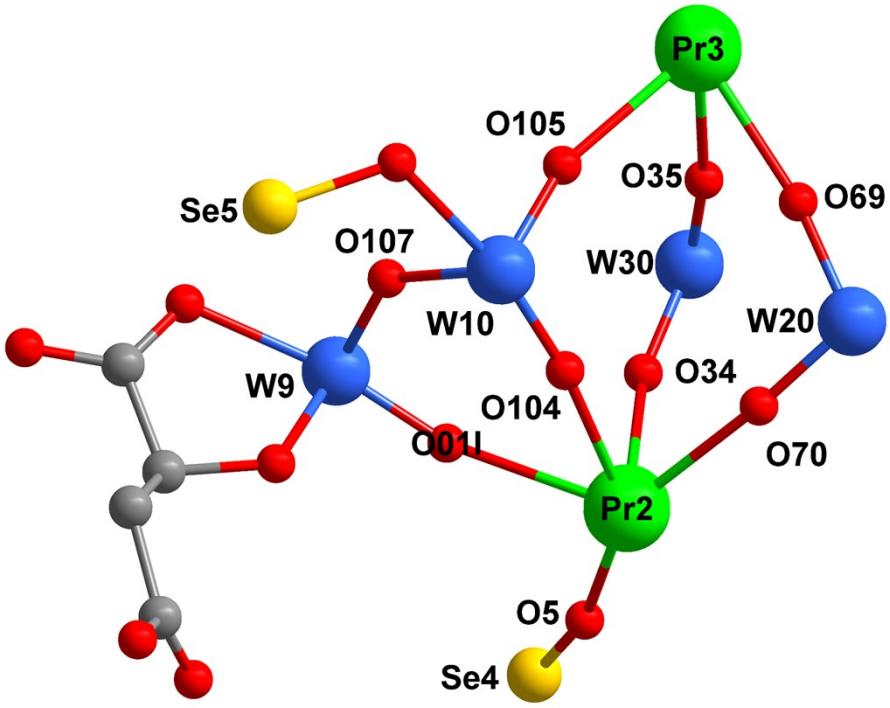

Figure S2. The structure of **BC-Pr**.

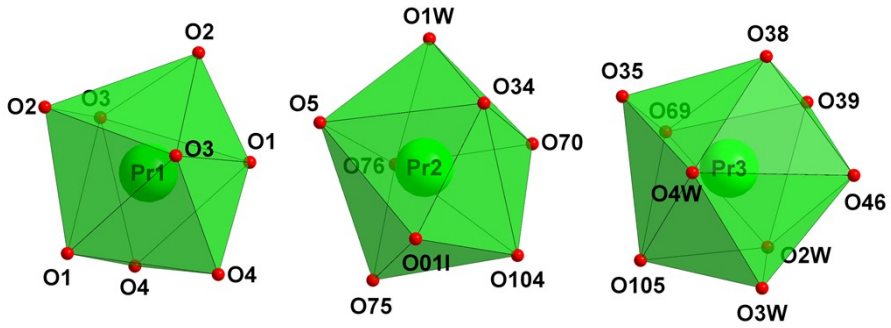

Figure S3. The coordination environment of Pr1, Pr2 and Pr3.

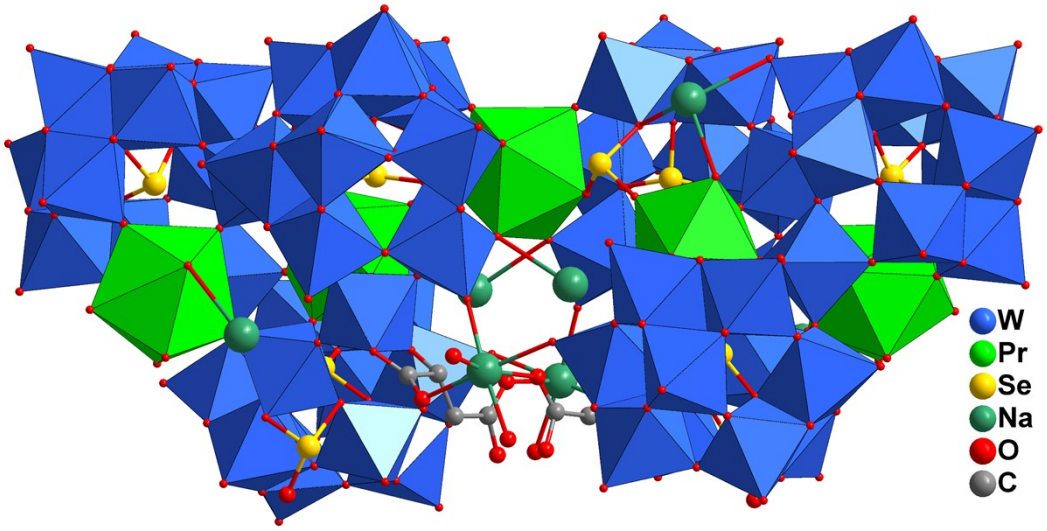

Figure S4. The dimer constructed by two clovers.

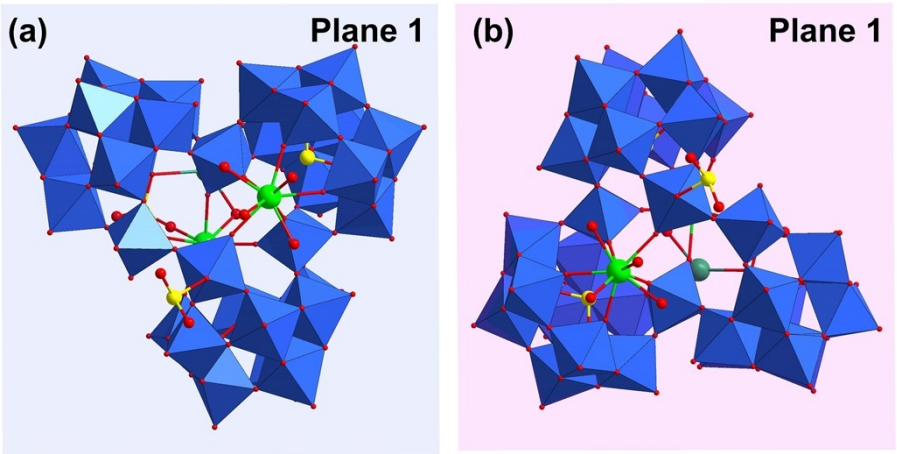

Figure S5. The planes constructed in **BC-Pr**.

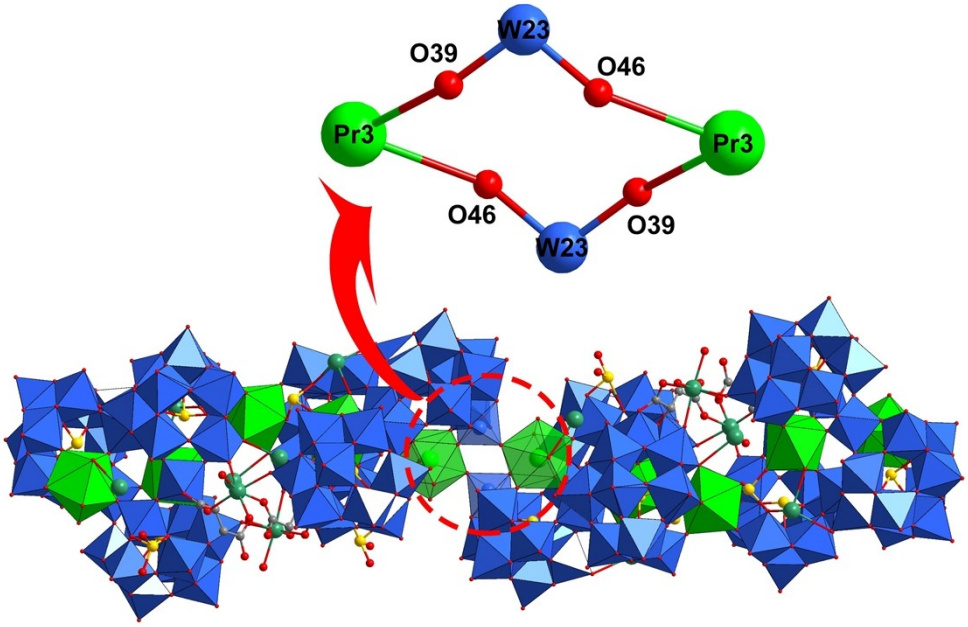

Figure S6. The connected mode in 1D chain.

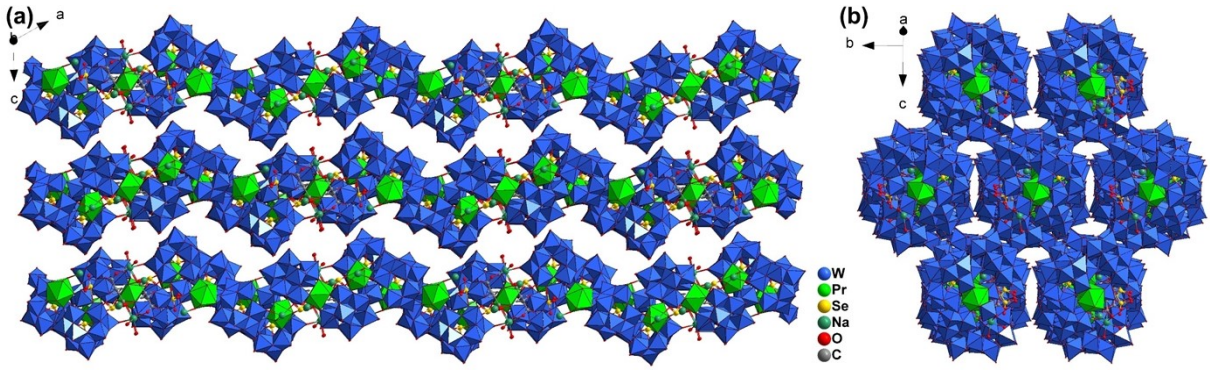

Figure S7. The three-dimensional supramolecular structure of **BC-Pr** from different directions.

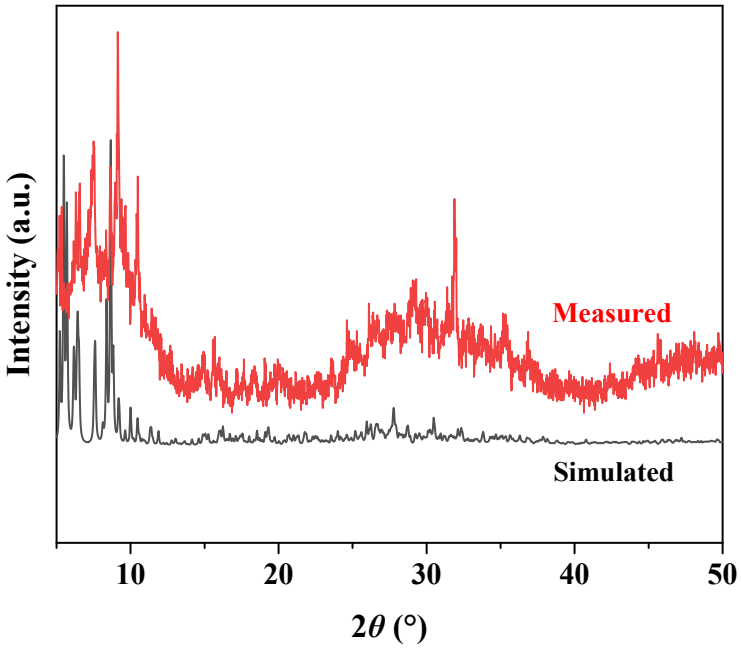

Figure S8. XRD pattern of **BC-Pr**.

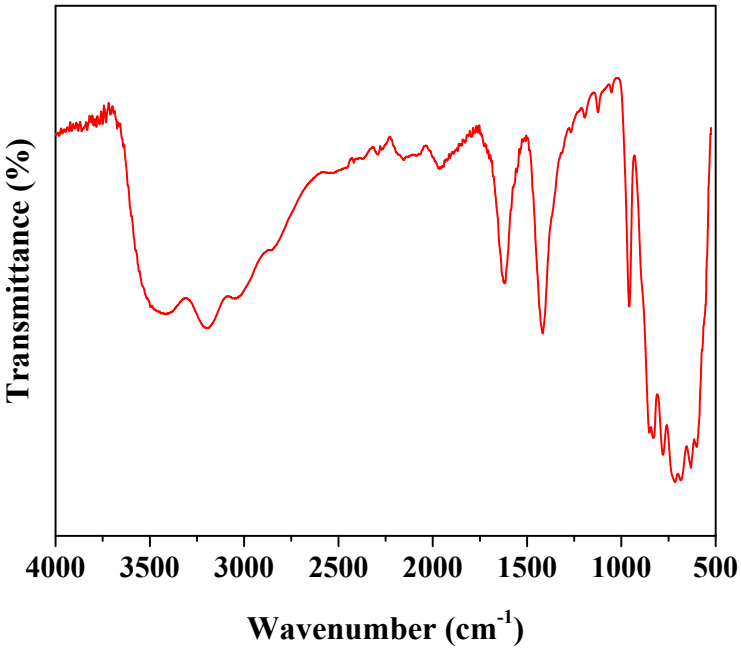

Figure S9. IR spectrum of **BC-Pr**.

4. Characterization of Products[4]

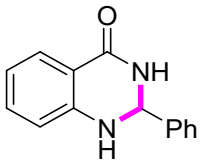

2-phenyl-2,3-dihydroquinazolin-4(1*H*)-one (3a)

EI-MS: $C_{14}H_{12}N_2O$, m/z (%) = 223.9 (44%) [M+].

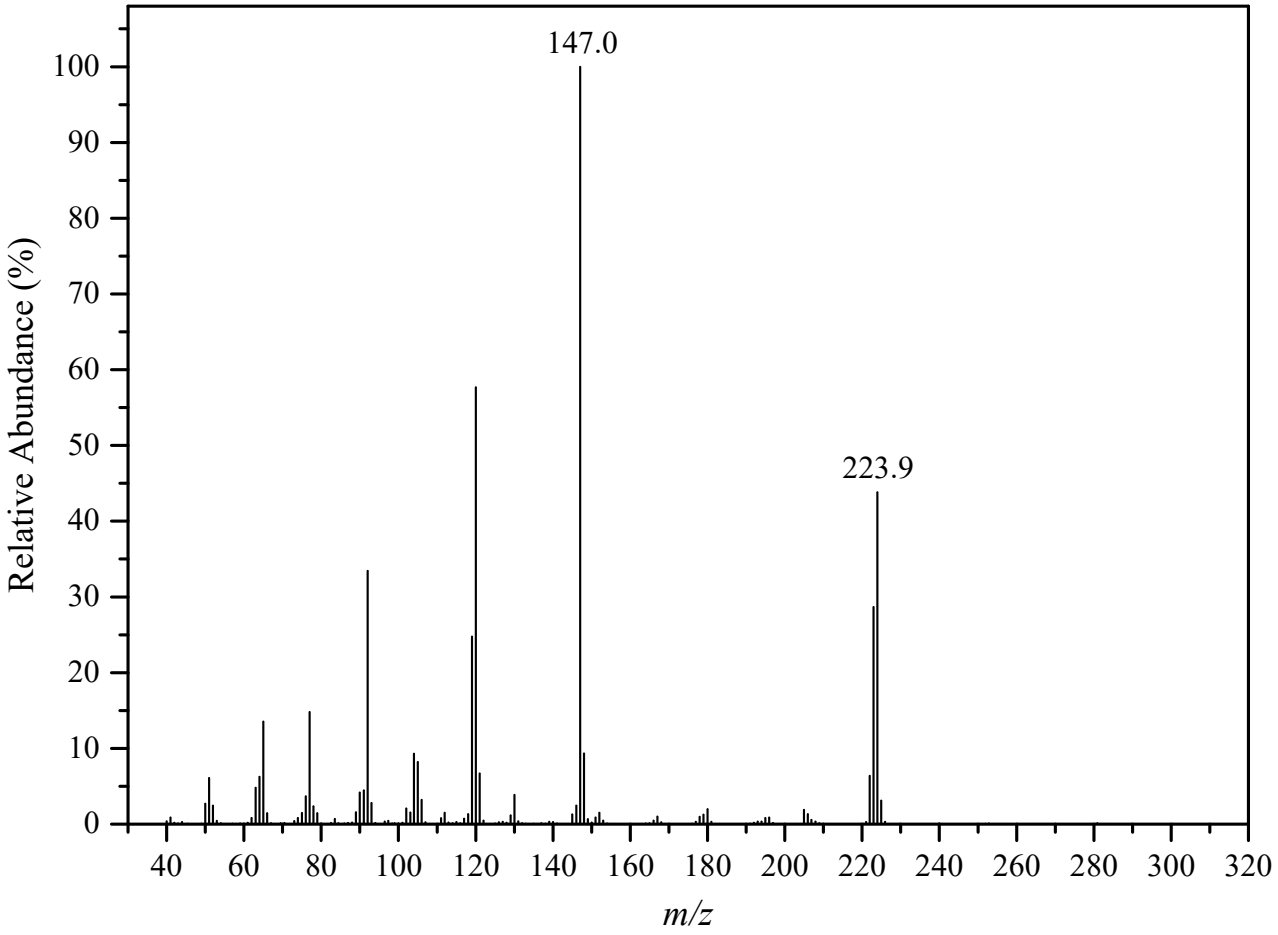

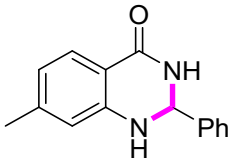

7-methyl-2-phenyl-2,3-dihydroquinazolin-4(1*H*)-one (3b)

EI-MS: $C_{15}H_{14}N_2O$, m/z (%) = 238.0 (43%) [M+].

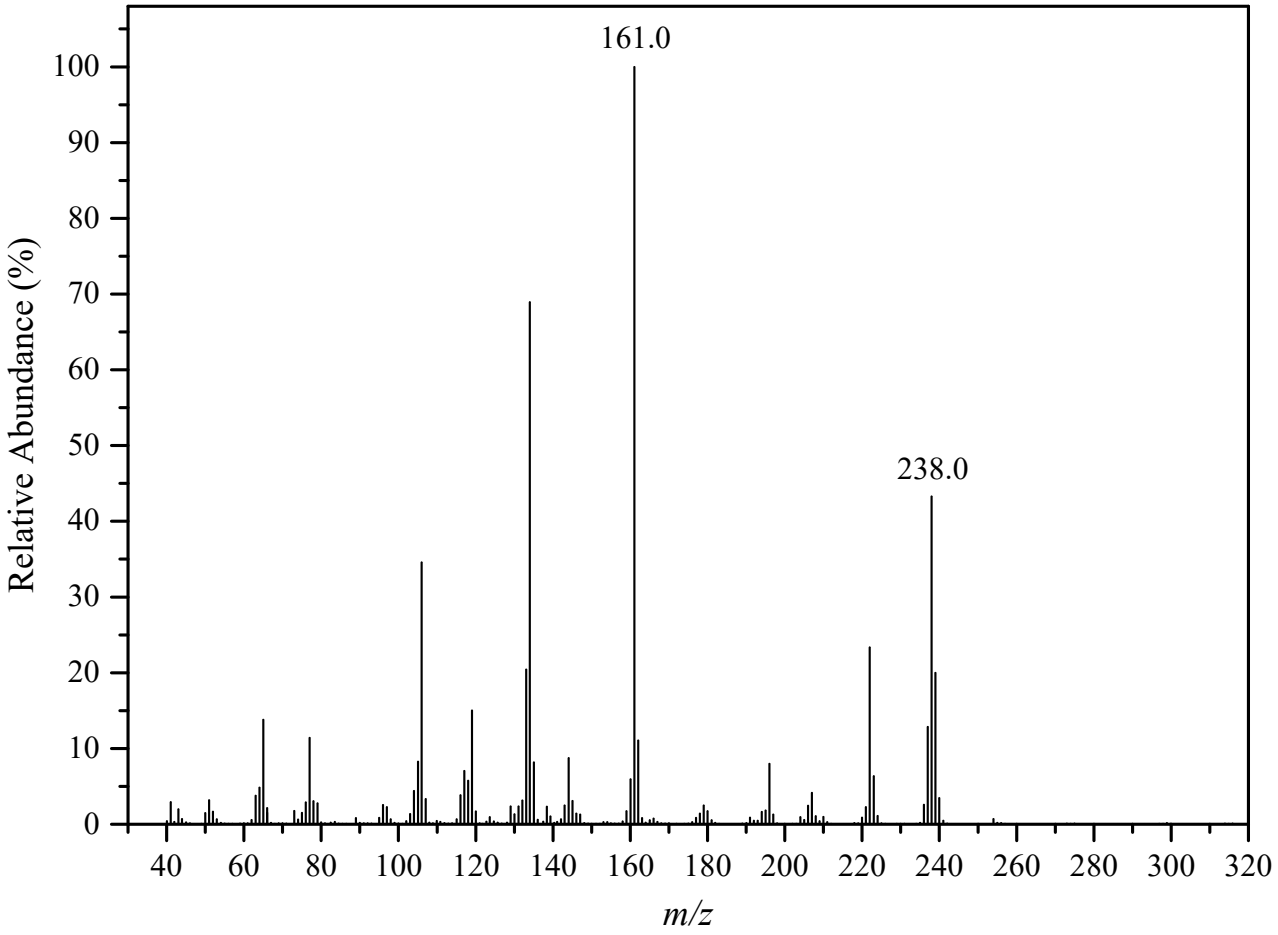

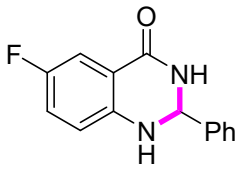

6-fluoro-2-phenyl-2,3-dihydroquinazolin-4(1*H*)-one (3c)

EI-MS: $C_{14}H_{11}FN_2O$, m/z (%) = 242.0 (31%) [M+].

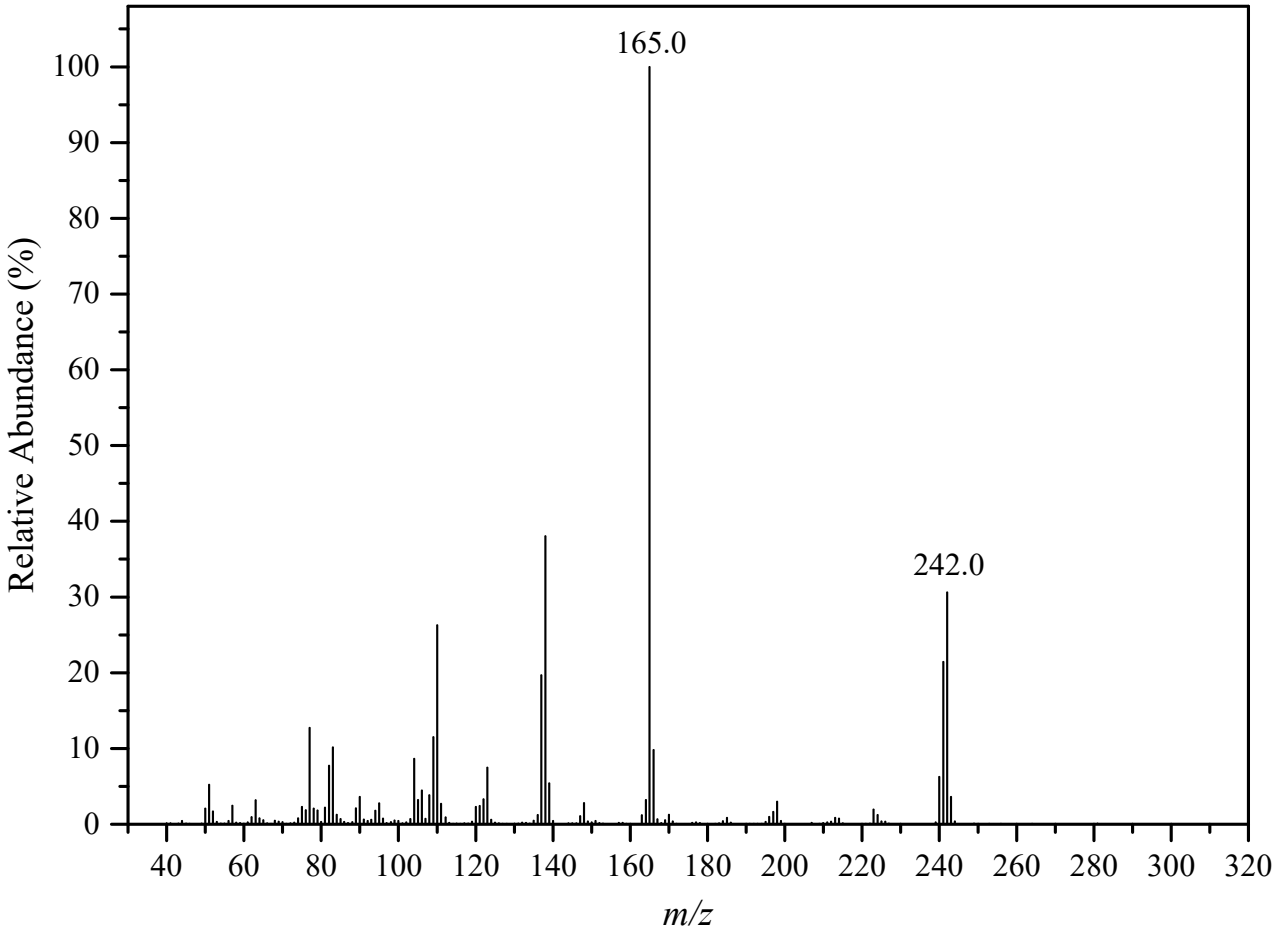

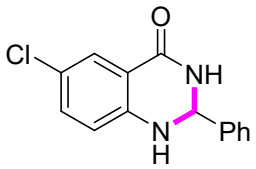

6-chloro-2-phenyl-2,3-dihydroquinazolin-4(1*H*)-one (3d)

EI-MS: $C_{14}H_{11}ClN_2O$, m/z (%) = 258.0 (24%) [M+].

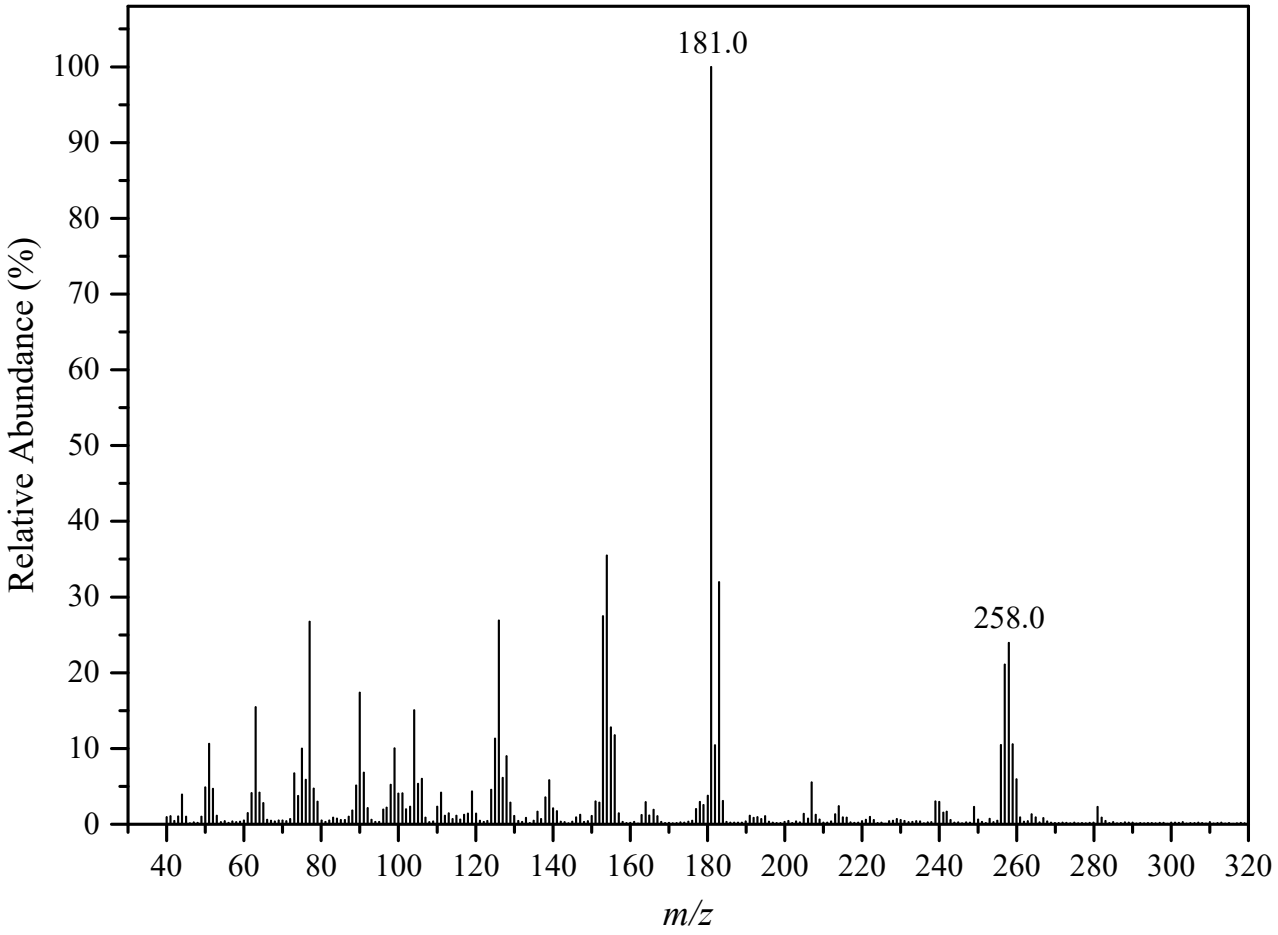

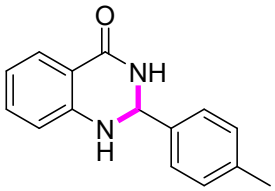

2-(*p*-tolyl)-2,3-dihydroquinazolin-4(1*H*)-one (3e)

EI-MS: $C_{15}H_{14}N_2O$, m/z (%) = 238.0 (50%) [M+].

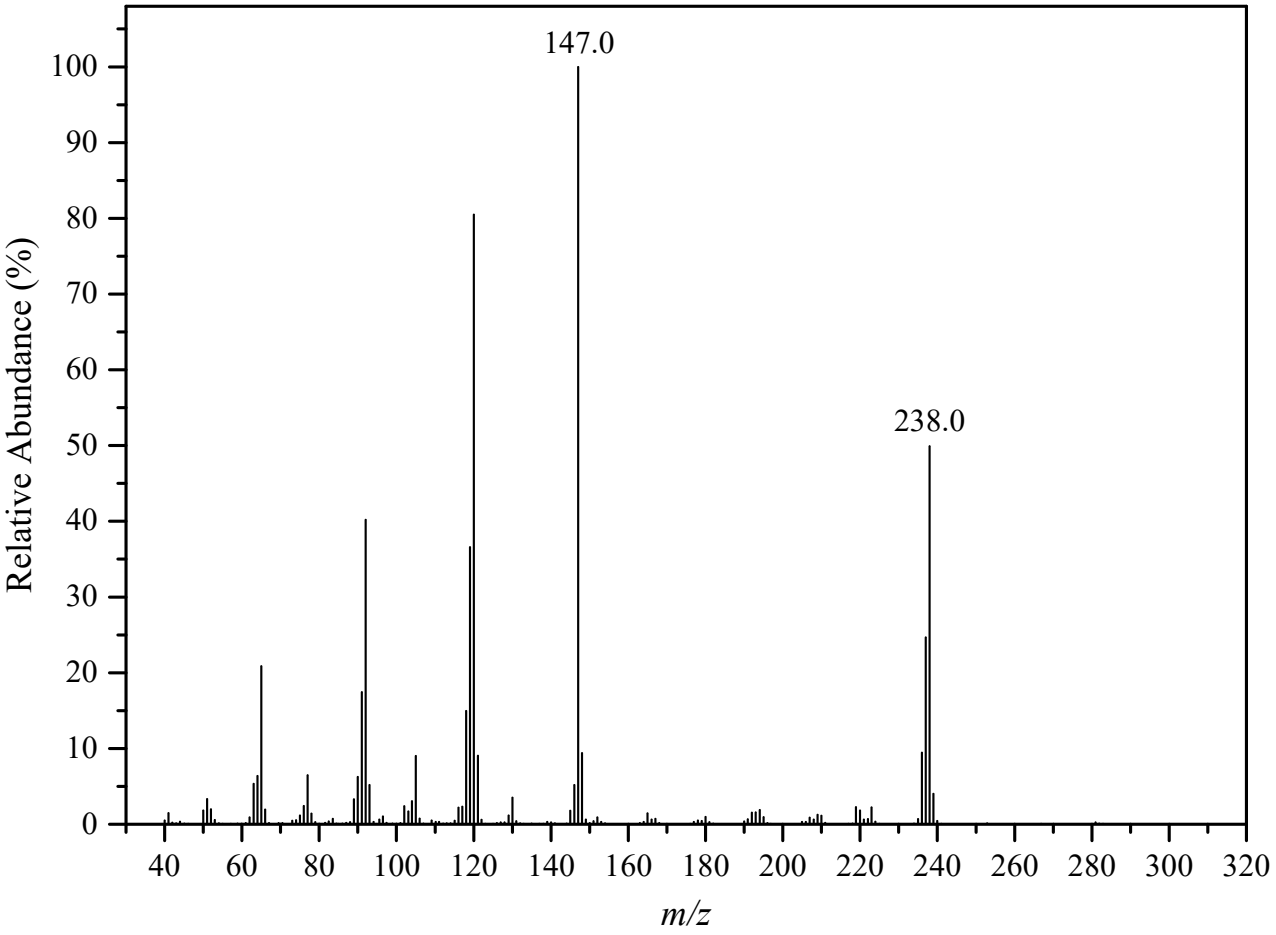

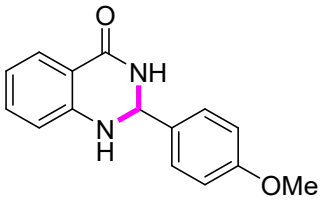

2-(4-methoxyphenyl)-2,3-dihydroquinazolin-4(1*H*)-one (3f)

EI-MS: $C_{15}H_{14}N_2O_2$, m/z (%) = 254.0 (48%) [M+].

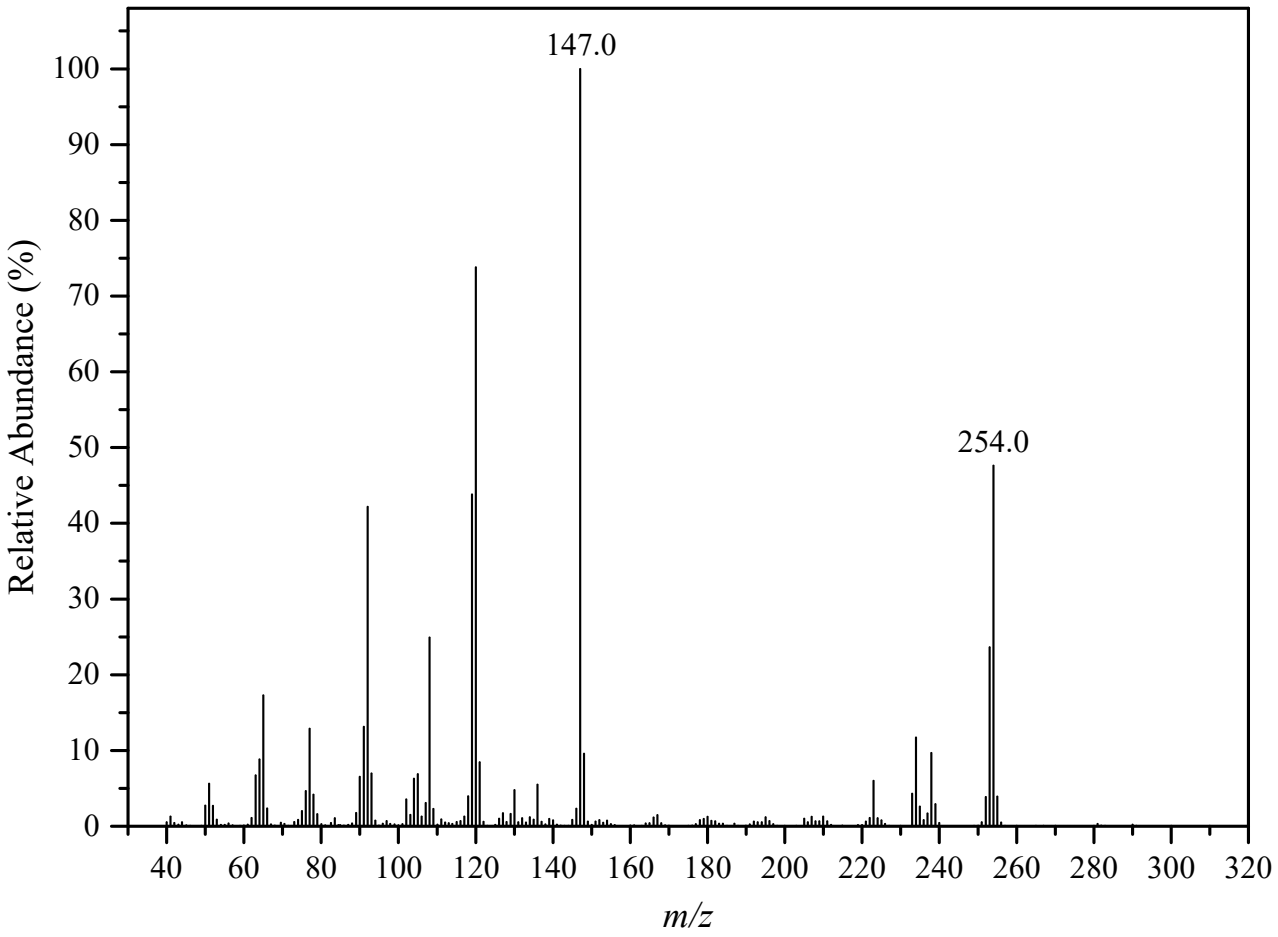

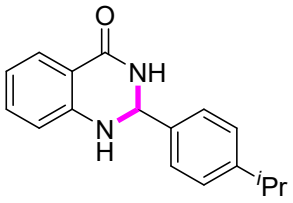

2-(4-isopropylphenyl)-2,3-dihydroquinazolin-4(1*H*)-one (3g)

EI-MS: $C_{17}H_{18}N_2O$, m/z (%) = 266.0 (39%) [M+].

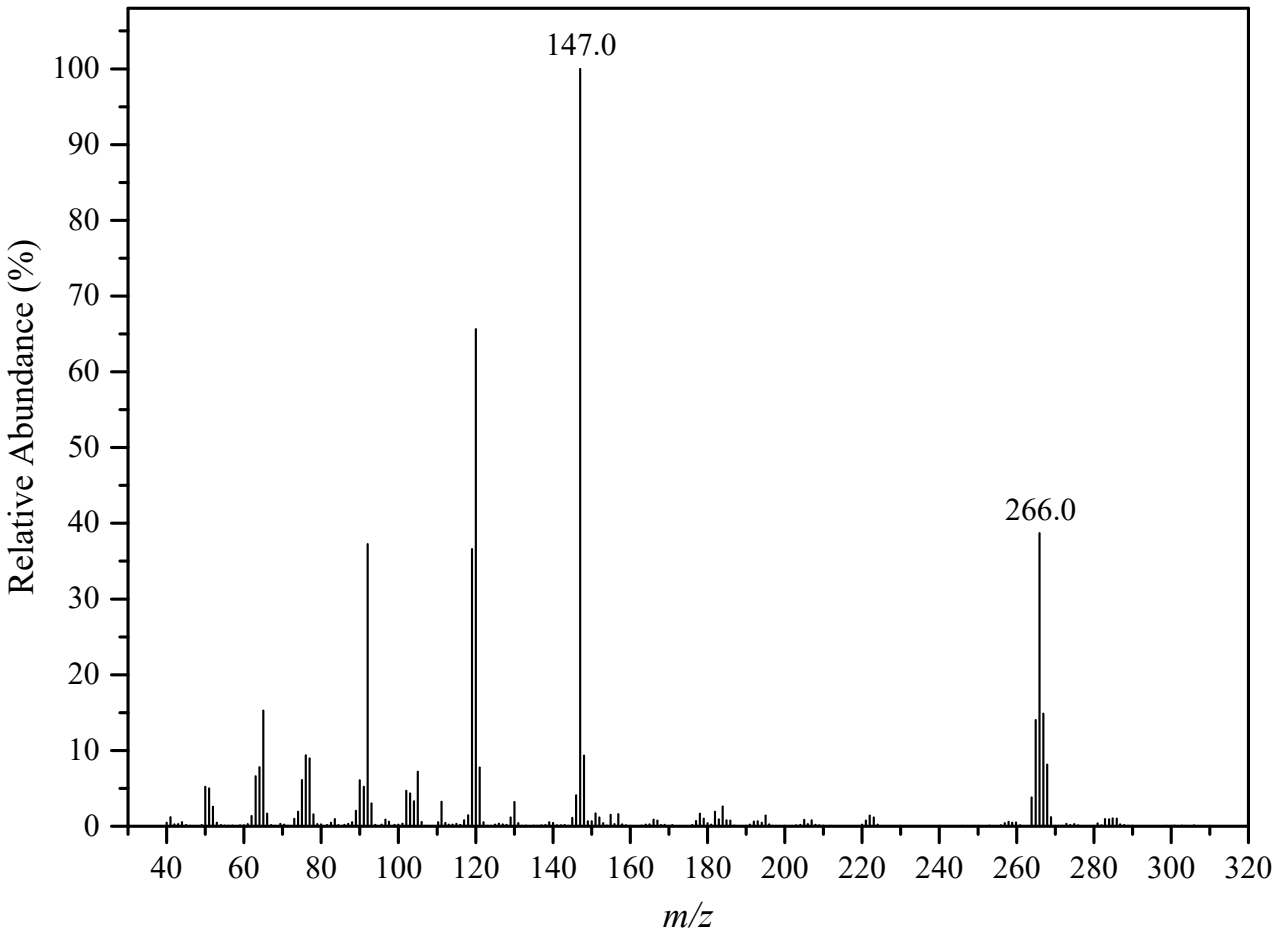

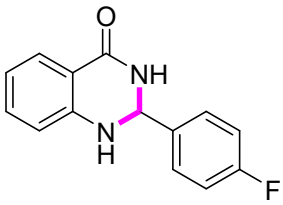

2-(4-fluorophenyl)-2,3-dihydroquinazolin-4(1*H*)-one (3h)

EI-MS: $C_{14}H_{11}FN_2O$, m/z (%) = 242.0 (36%) [M+].

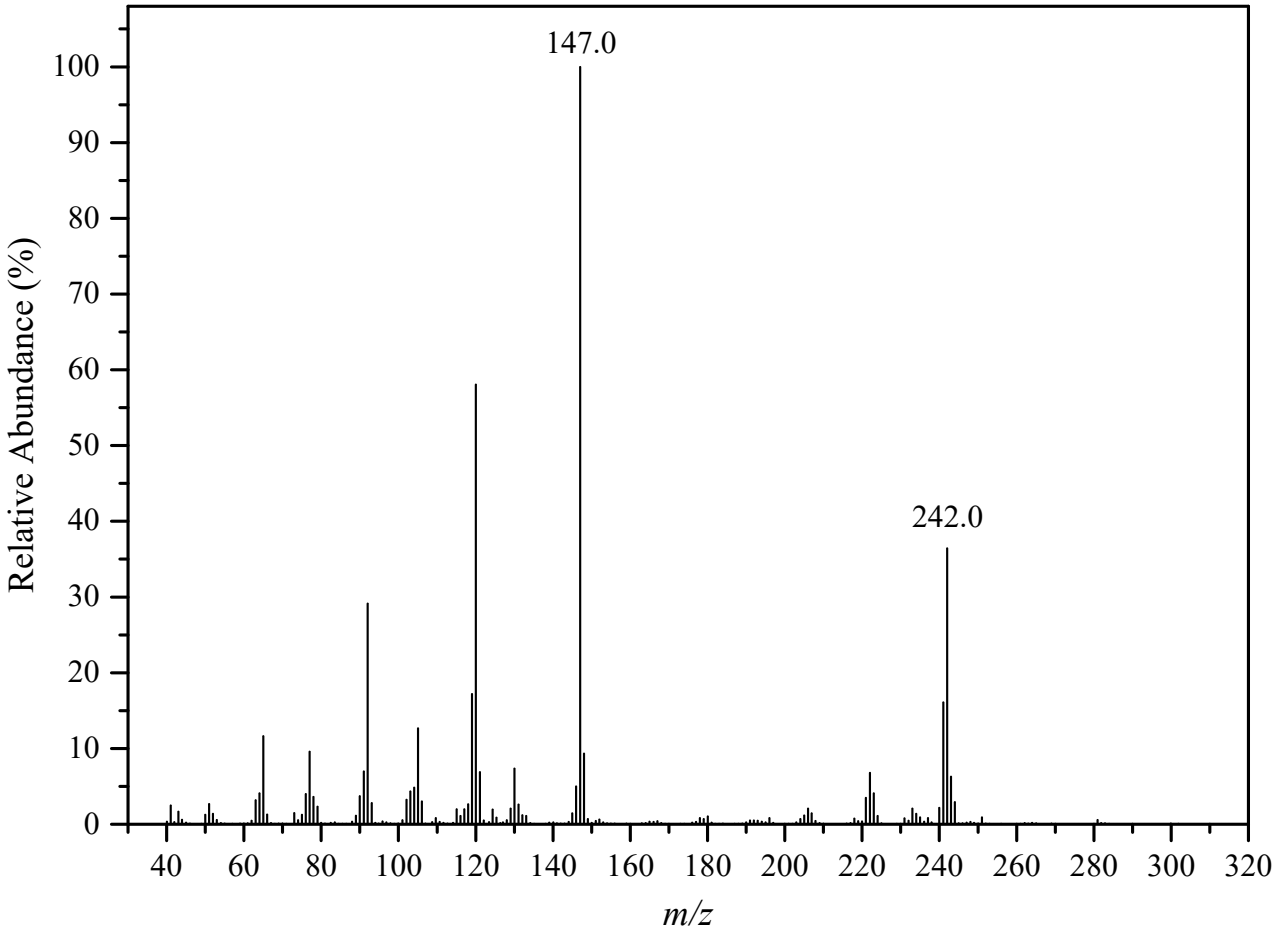

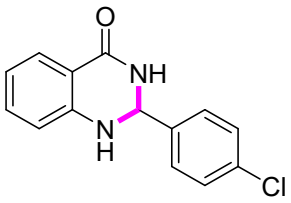

2-(4-chlorophenyl)-2,3-dihydroquinazolin-4(1*H*)-one (3i)

EI-MS: $C_{14}H_{11}ClN_2O$, m/z (%) = 258.0 (18%) [M+].

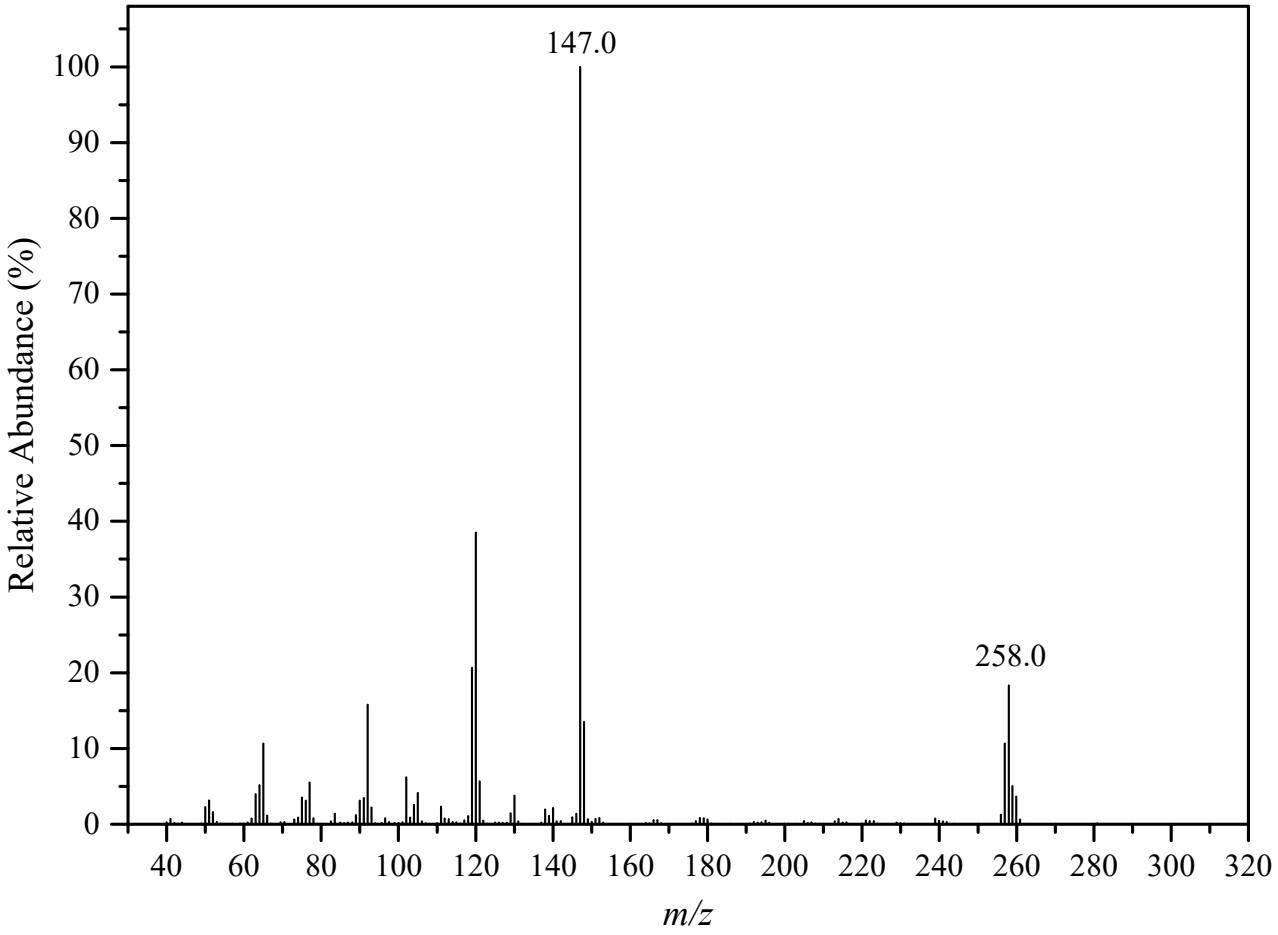

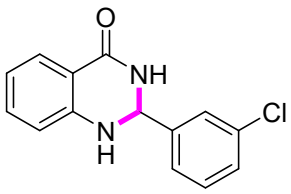

2-(3-chlorophenyl)-2,3-dihydroquinazolin-4(1*H*)-one (3j)

EI-MS: $C_{14}H_{11}ClN_2O$, m/z (%) = 258.0 (22%) [M+].

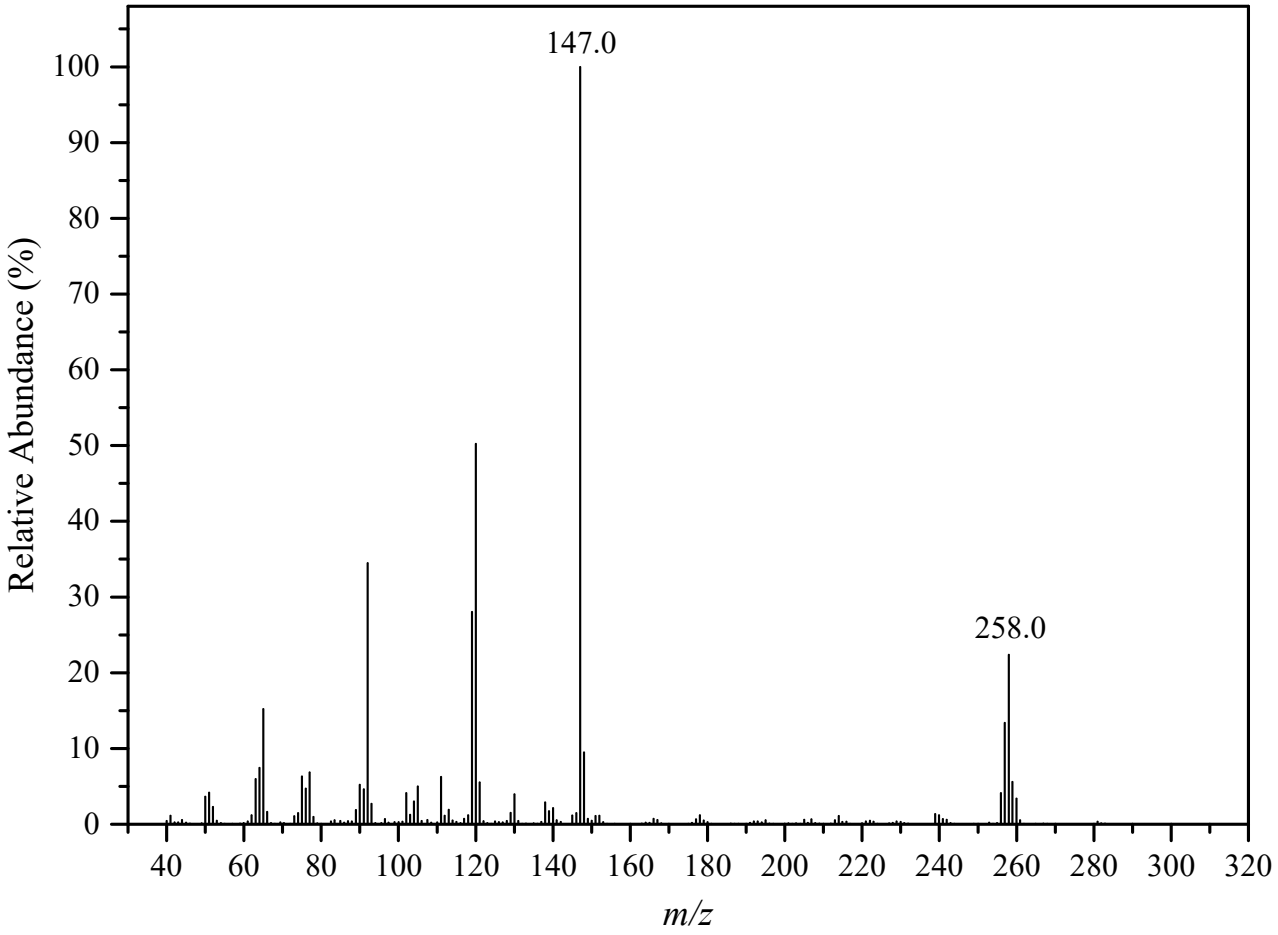

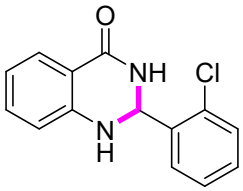

2-(2-chlorophenyl)-2,3-dihydroquinazolin-4(1*H*)-one (3k)

EI-MS: $C_{14}H_{11}ClN_2O$, m/z (%) = 258.0 (22%) [M+].

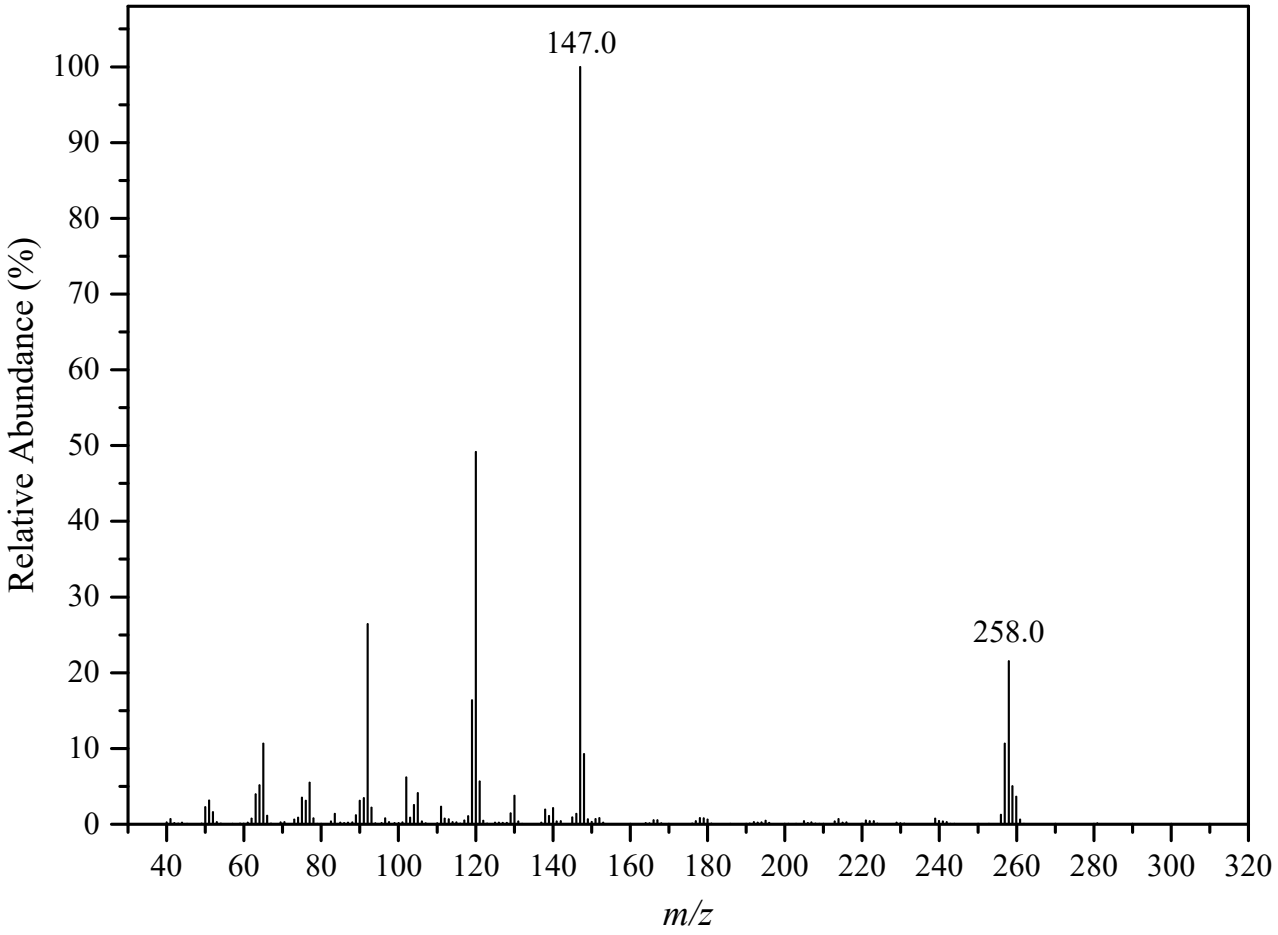

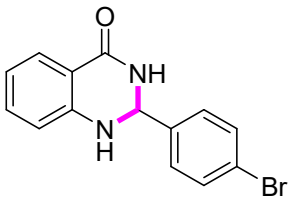

2-(4-bromophenyl)-2,3-dihydroquinazolin-4(1*H*)-one (3l)

EI-MS: $C_{14}H_{11}BrN_2O$, m/z (%) = 302.0 (37%) [M+].

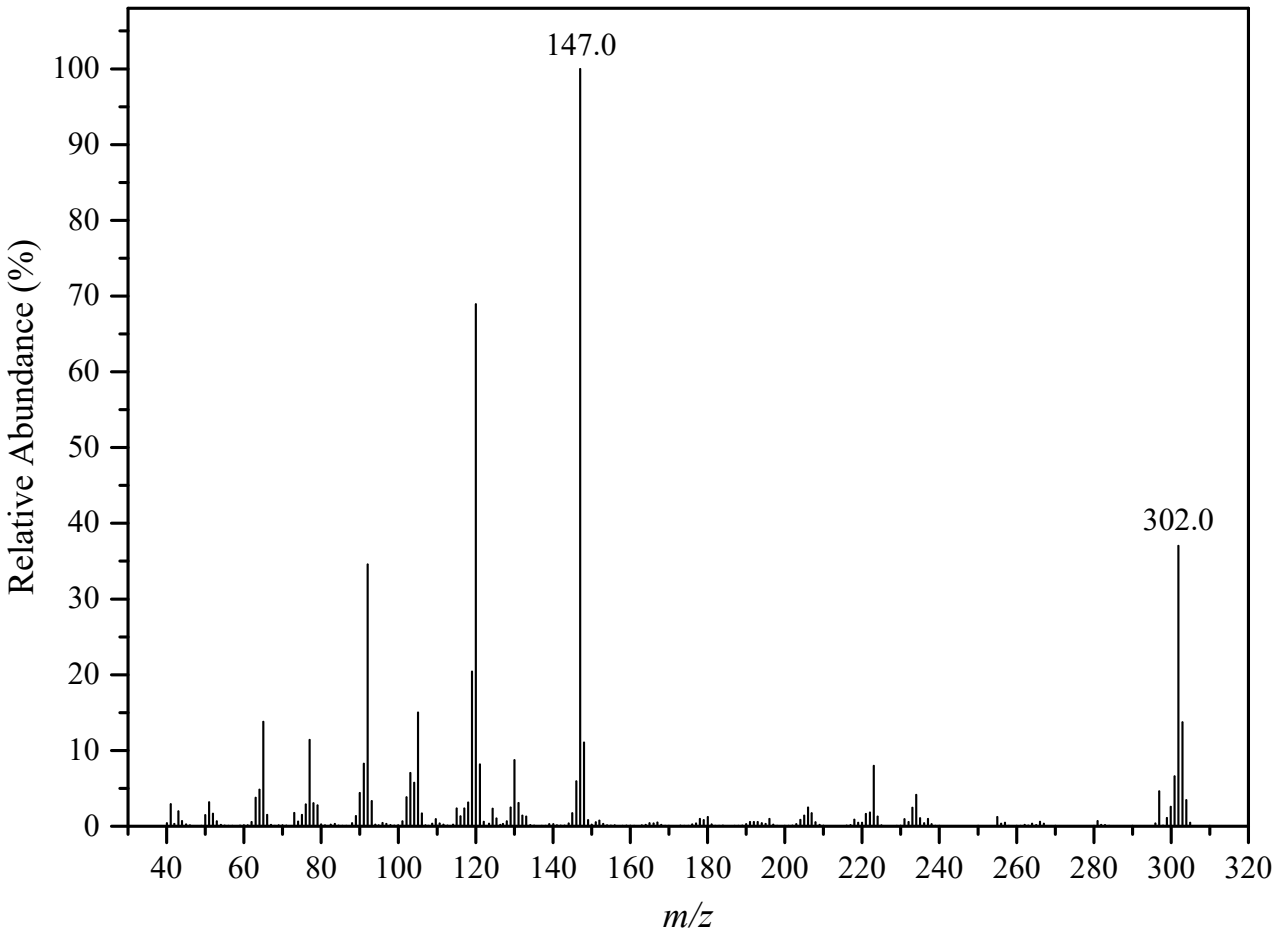

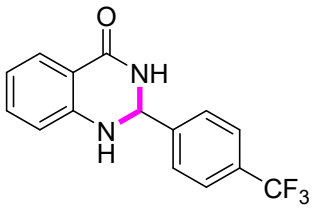

2-(4-(trifluoromethyl)phenyl)-2,3-dihydroquinazolin-4(1*H*)-one (3m)

EI-MS: $C_{15}H_{11}F_3N_2O$, m/z (%) = 292.0 (22%) [M+].

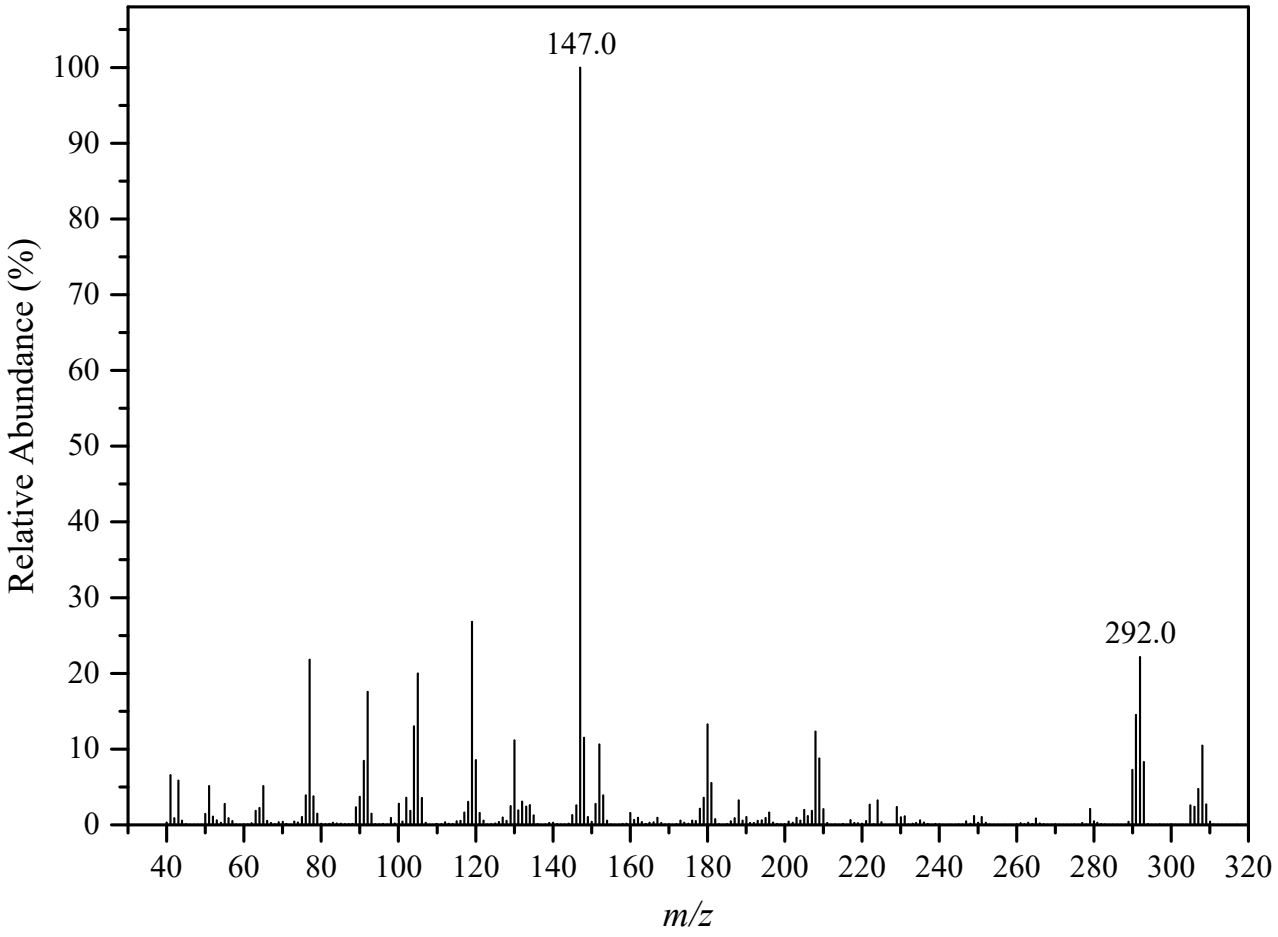

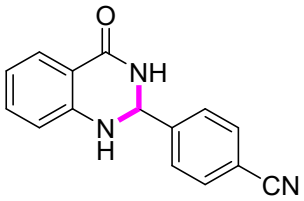

4-(4-oxo-1,2,3,4-tetrahydroquinazolin-2-yl)benzonitrile (3n)

EI-MS: $C_{15}H_{11}N_3O$, m/z (%) = 249.0 (24%) [M+].

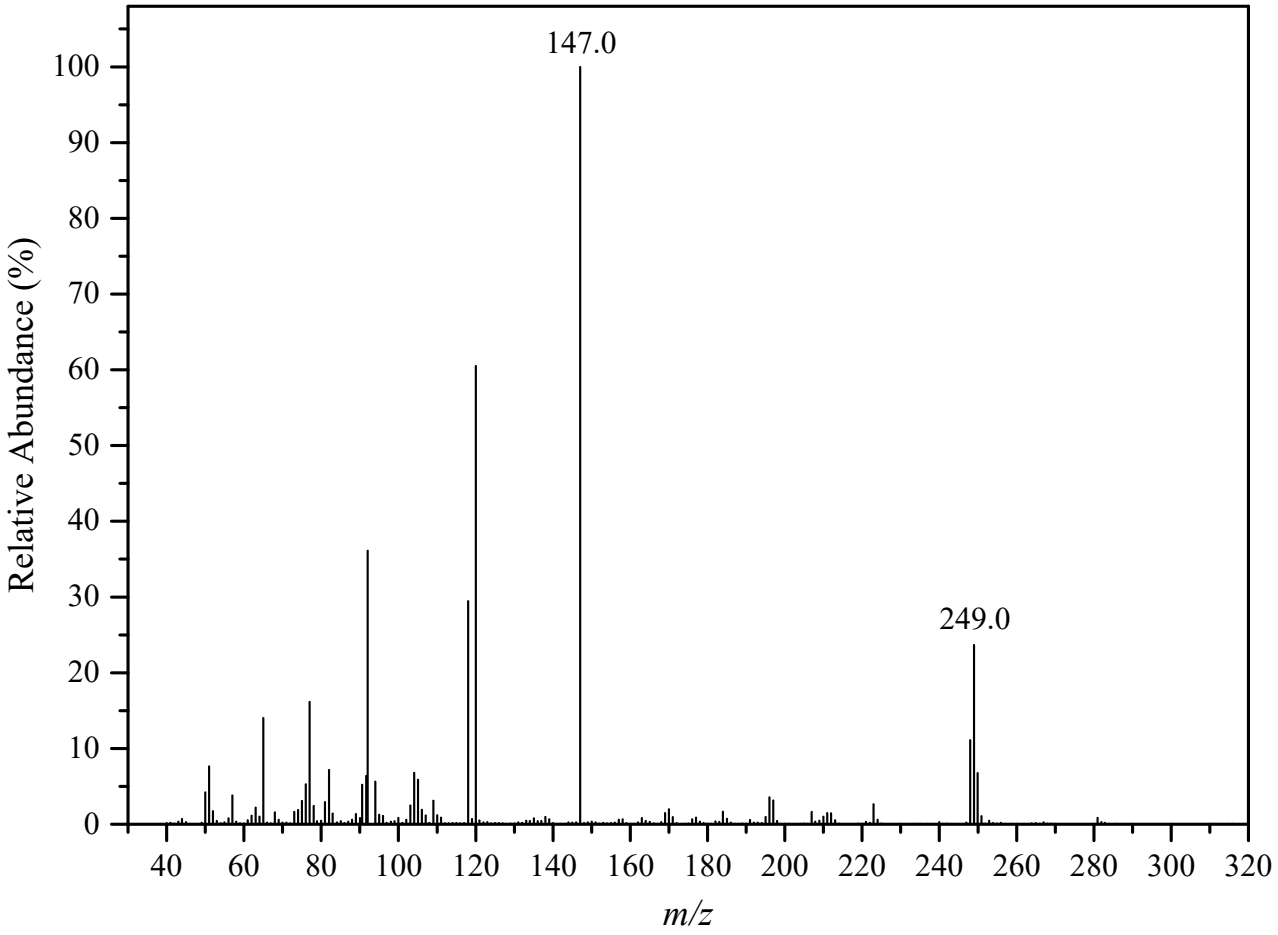

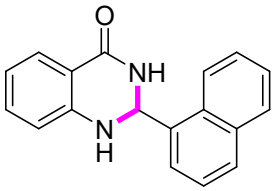

2-(naphthalen-1-yl)-2,3-dihydroquinazolin-4(1*H*)-one (3o)

EI-MS: $C_{18}H_{14}N_2O$, m/z (%) = 274.0 (30%) [M+].

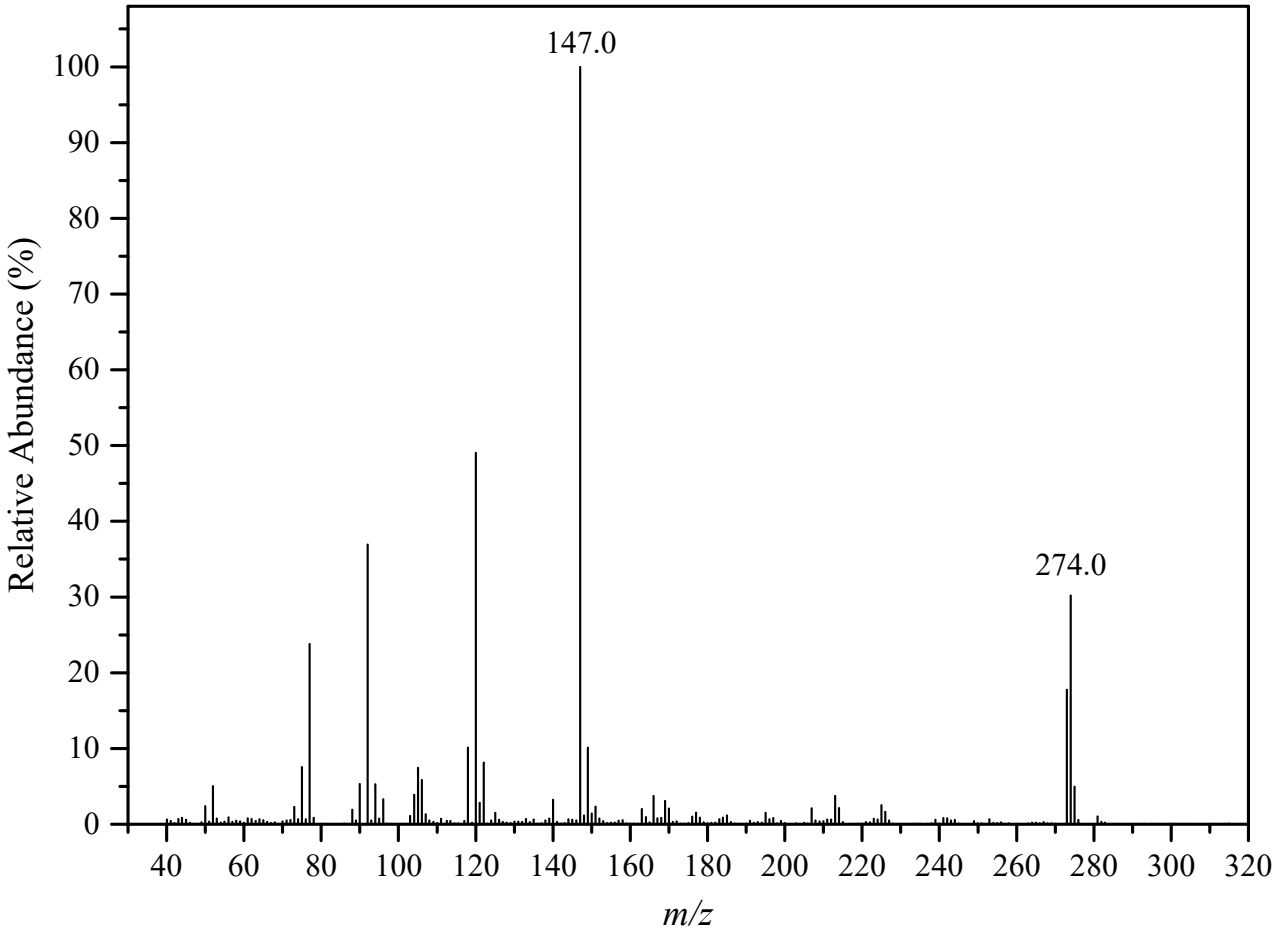

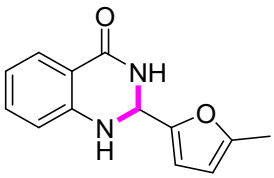

2-(5-methylfuran-2-yl)-2,3-dihydroquinazolin-4(1*H*)-one (3p)

EI-MS: $C_{13}H_{12}N_2O_2$, m/z (%) = 228.0 (31%) [M+].

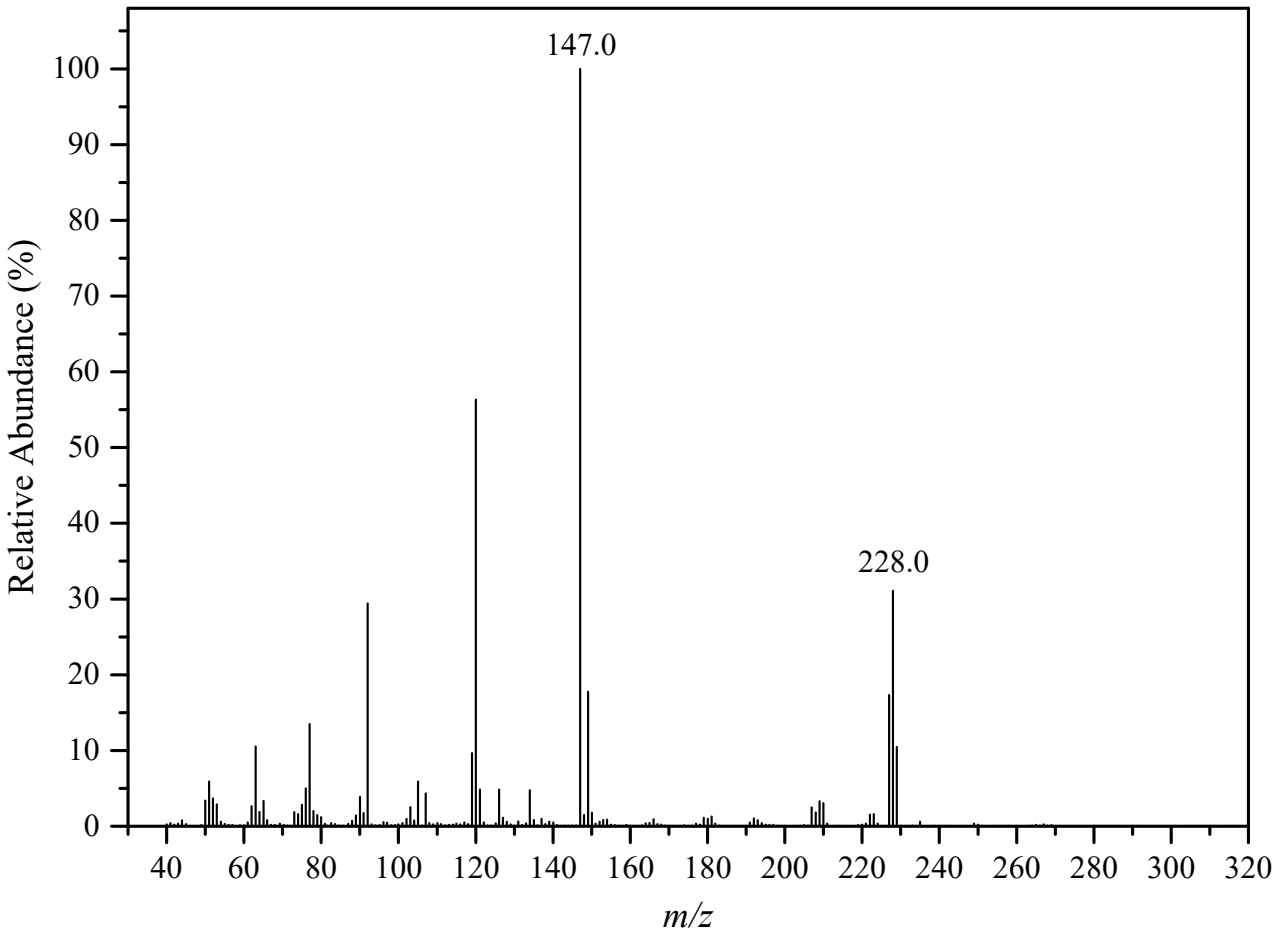

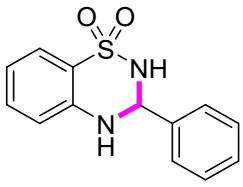

3-phenyl-3,4-dihydro-2*H*-benzo[e][1,2,4]thiadiazine 1,1-dioxide (5a)

EI-MS: $C_{13}H_{12}N_2O_2S$, m/z (%) = 260.1 (16%) [M+].

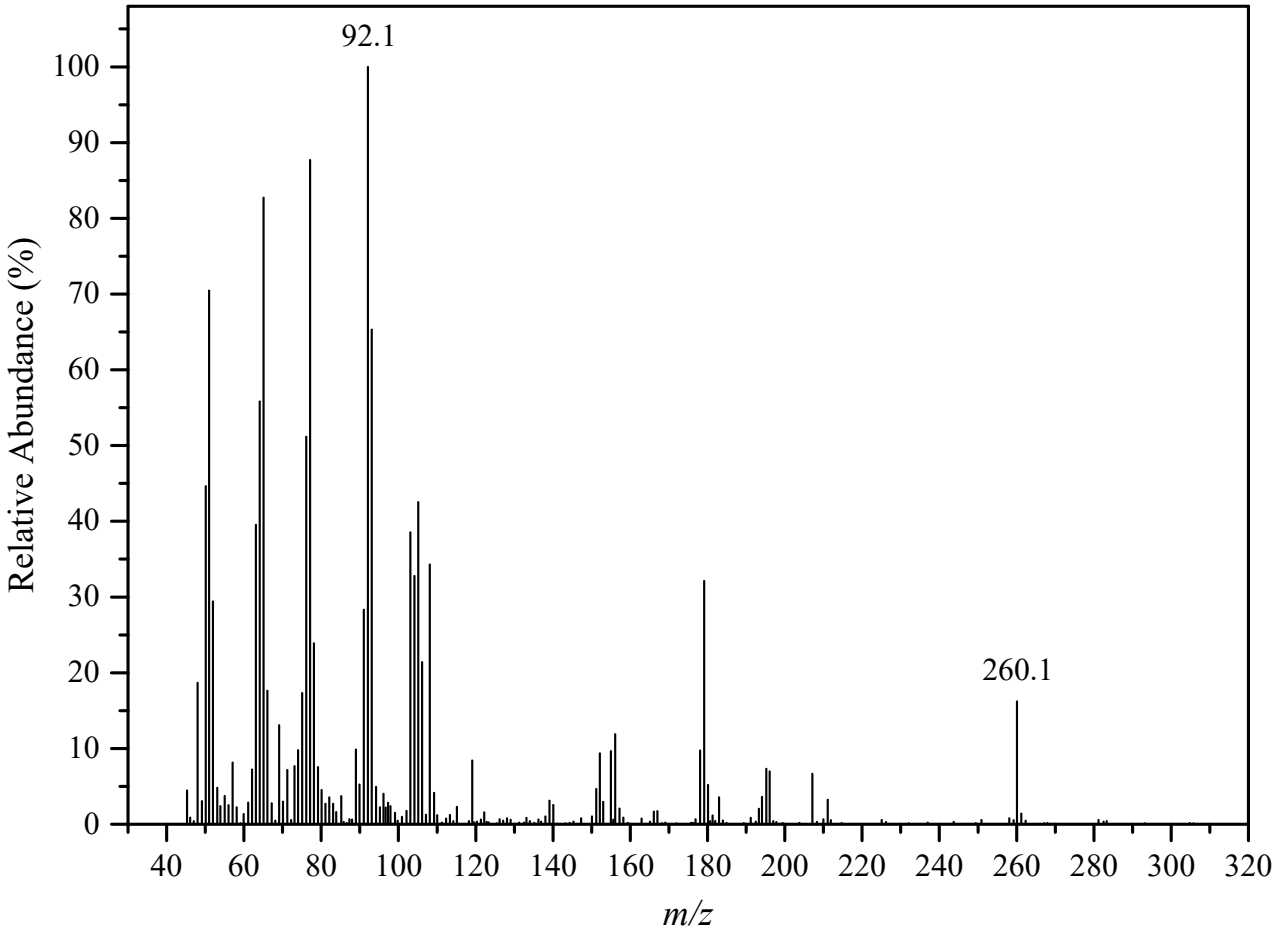

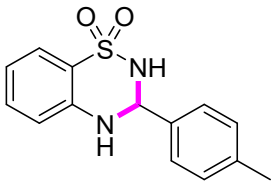

3-(o-tolyl)-3,4-dihydro-2*H*-benzo[e][1,2,4]thiadiazine 1,1-dioxide (5b)

EI-MS: $C_{14}H_{14}N_2O_2S$, m/z (%) = 274.1 (16%) [M+].

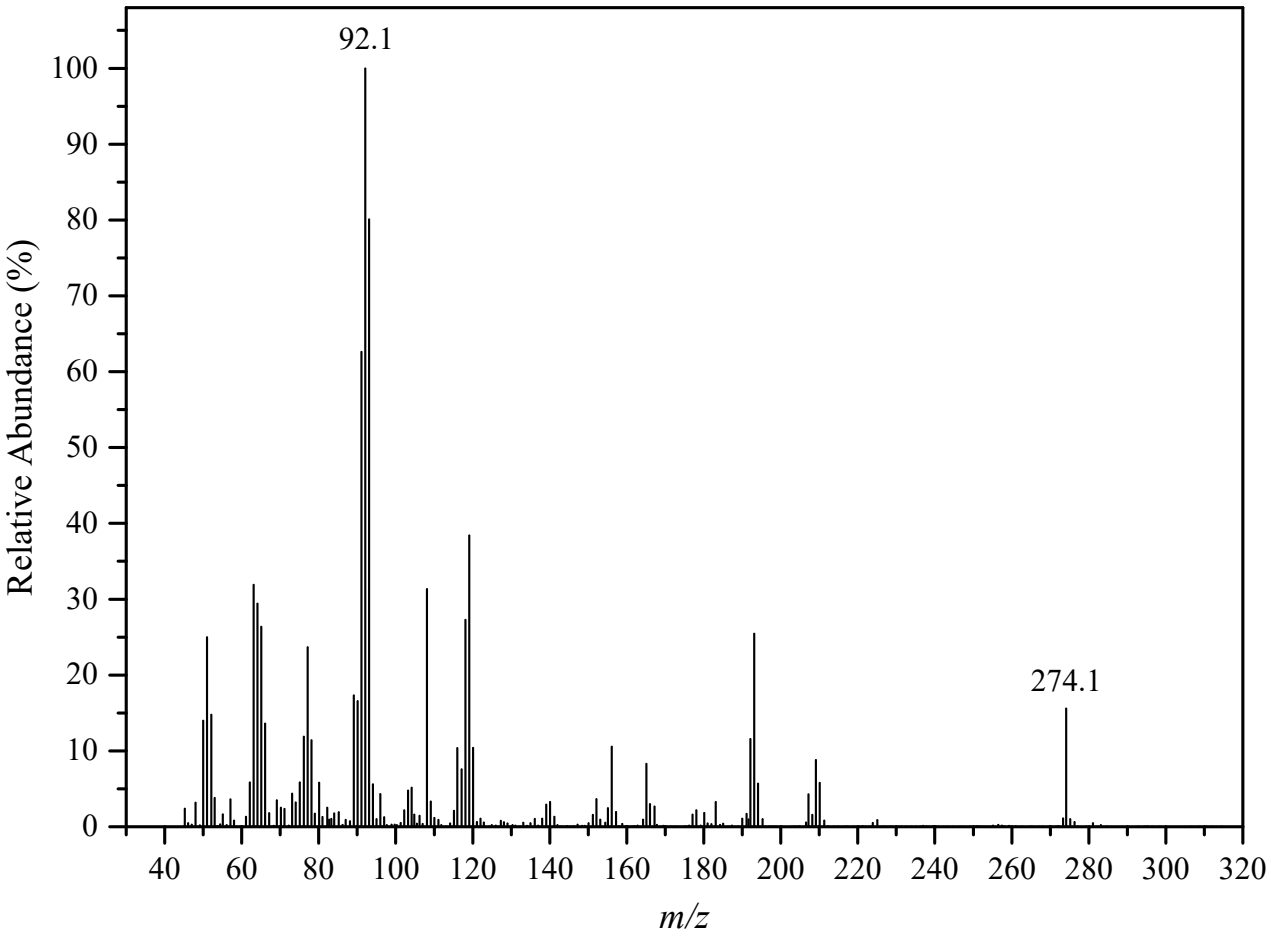

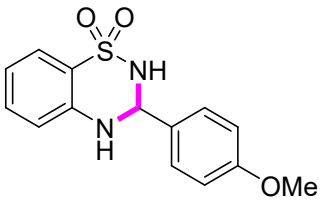

3-(4-methoxyphenyl)-3,4-dihydro-2*H*-benzo[e][1,2,4]thiadiazine 1,1-dioxide (5c)

EI-MS: $C_{14}H_{14}N_2O_3S$, m/z (%) = 290.1 (11%) [M+].

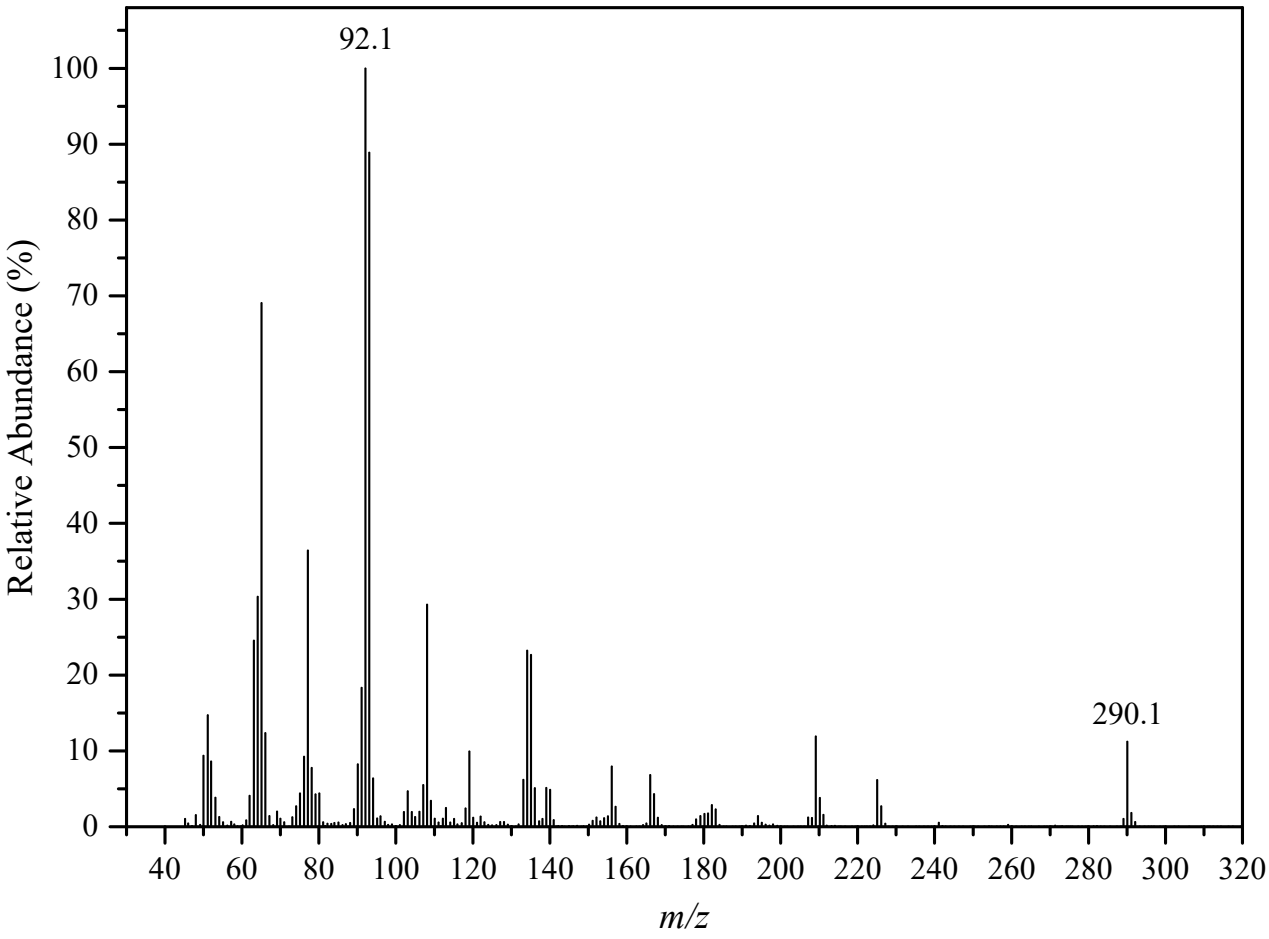

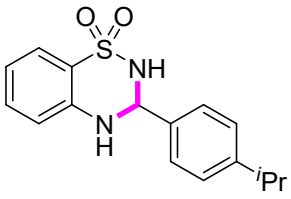

3-(4-isopropylphenyl)-3,4-dihydro-2*H*-benzo[e][1,2,4]thiadiazine 1,1-dioxide (5d)

EI-MS: $C_{16}H_{18}N_2O_2S$, m/z (%) = 302.1 (10%) [M+].

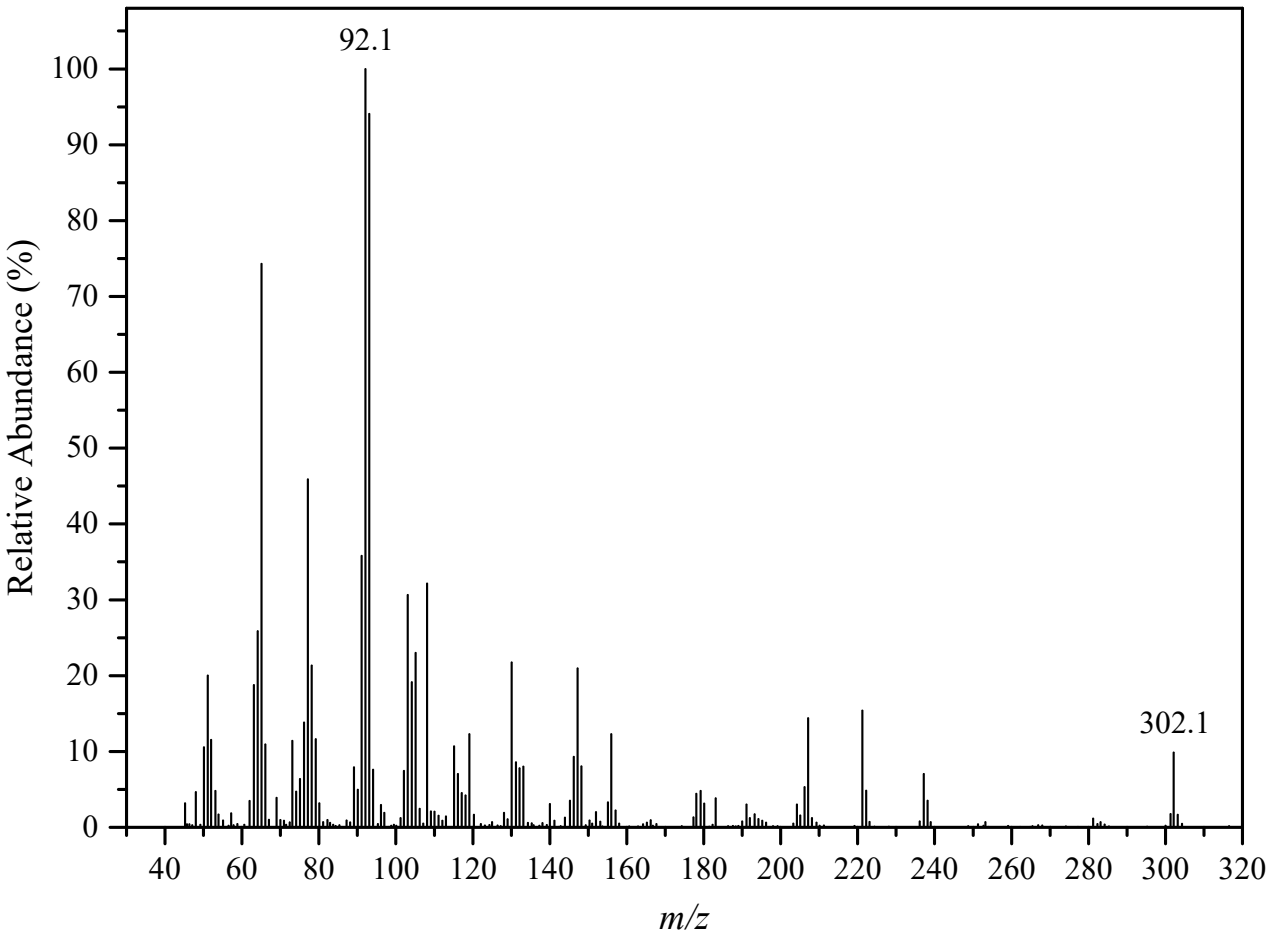

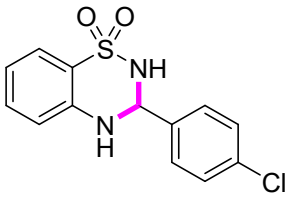

3-(4-chlorophenyl)-3,4-dihydro-2H-benzo[e][1,2,4]thiadiazine 1,1-dioxide (5e)

EI-MS: $C_{13}H_{11}ClN_2O_2S$, m/z (%) = 294.1 (6%) [M+].

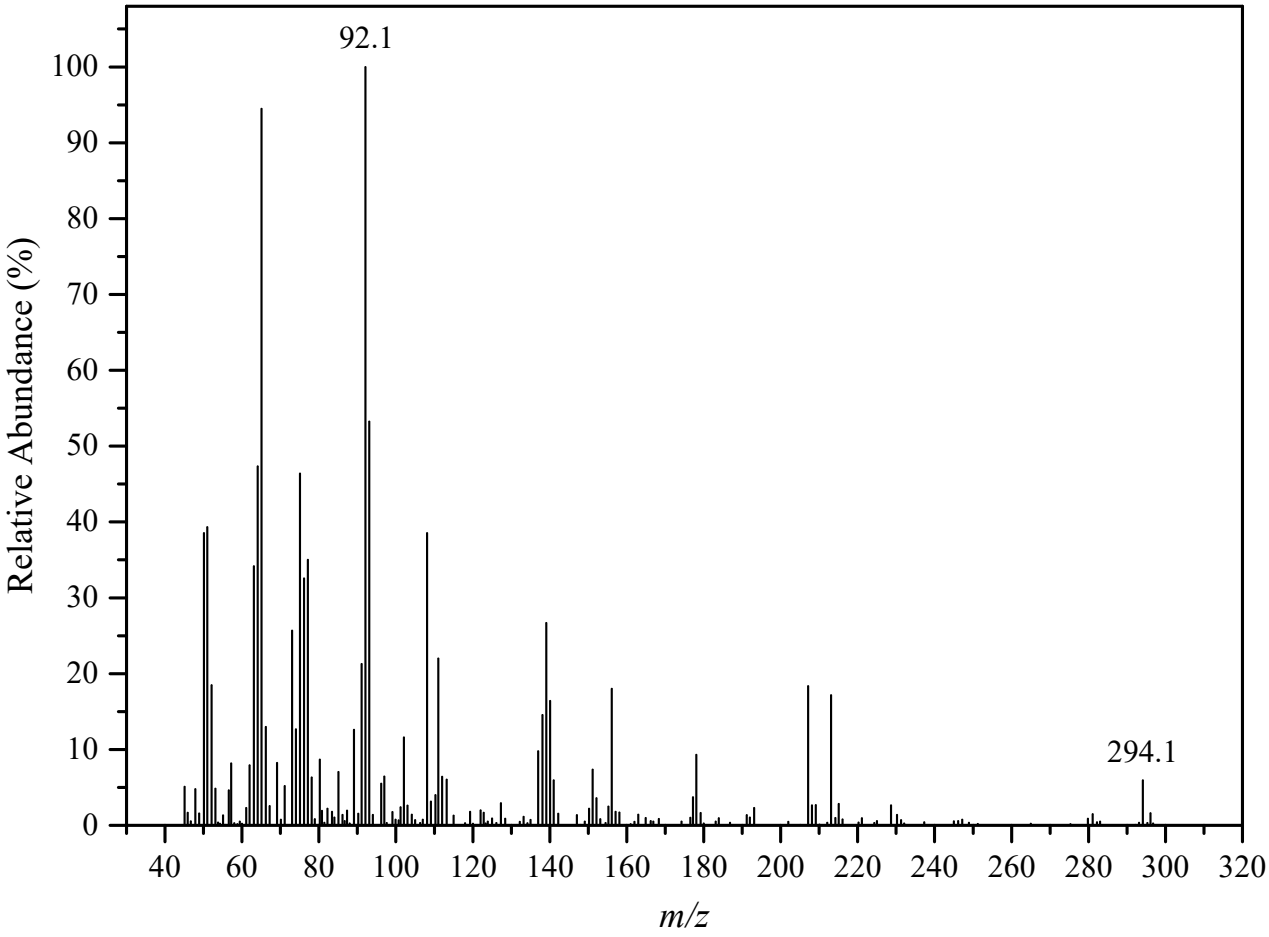

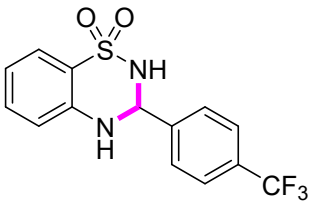

3-(4-(trifluoromethyl)phenyl)-3,4-dihydro-2*H*-benzo[e][1,2,4]thiadiazine 1,1-dioxide (5f)

EI-MS: $C_{14}H_{11}F_3N_2O_2S$, m/z (%) = 328.0 (12%) [M+].

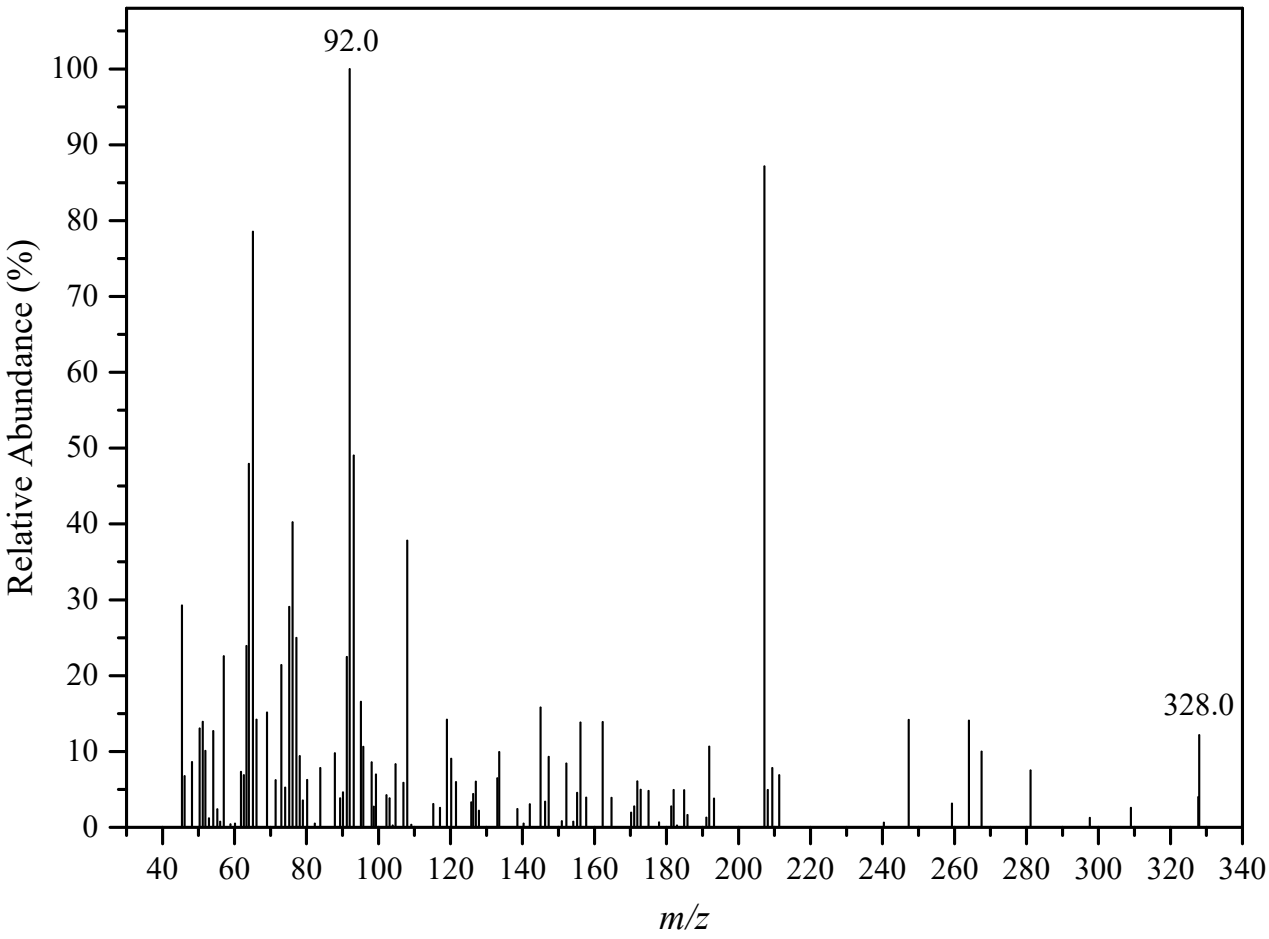

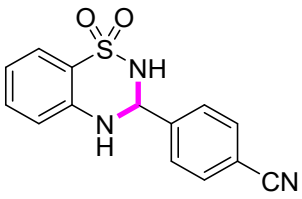

4-(1,1-dioxido-3,4-dihydro-2*H*-benzo[e][1,2,4]thiadiazin-3-yl)benzonitrile (5g)

EI-MS: $C_{14}H_{11}ClN_3O_2S$, m/z (%) = 285.1 (10%) [M+].

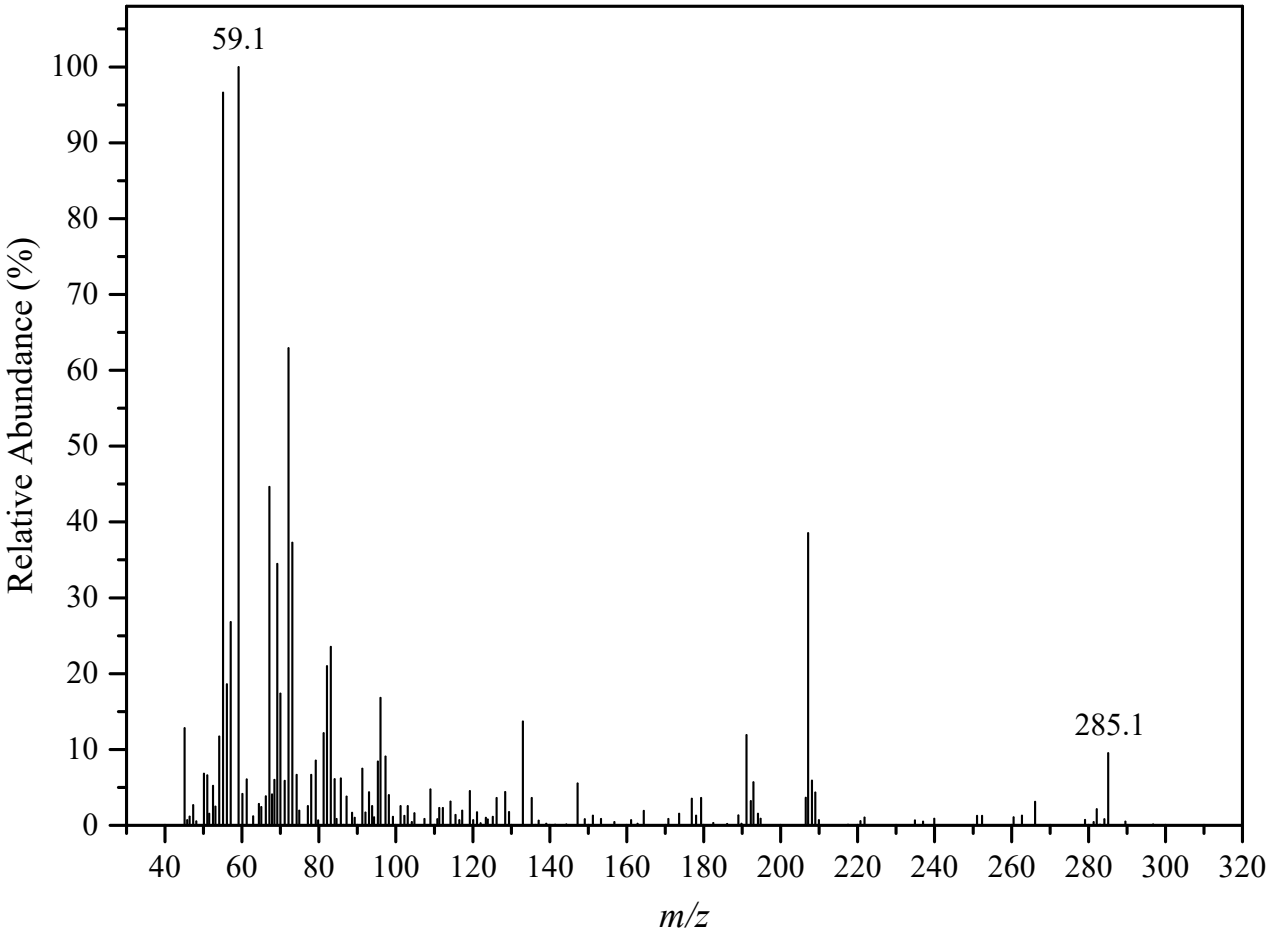

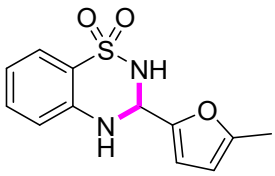

3-(5-methylfuran-2-yl)-3,4-dihydro-2*H*-benzo[e][1,2,4]thiadiazine 1,1-dioxide (5h)

EI-MS: $C_{12}H_{12}N_2O_3S$, m/z (%) =264.1 (18%) [M+].

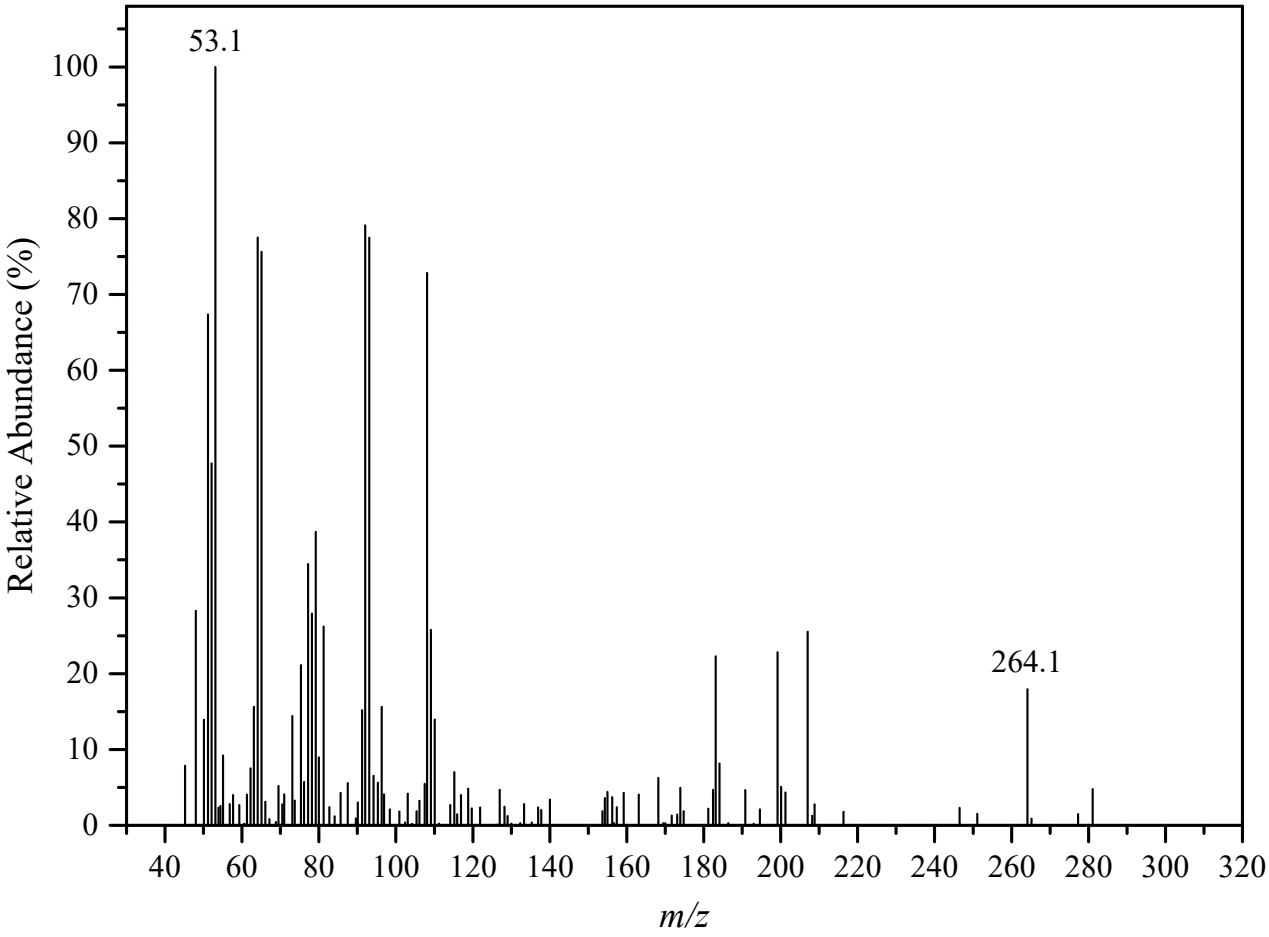

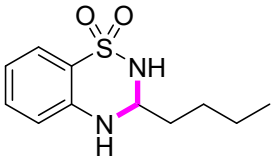

3-butyl-3,4-dihydro-2*H*-benzo[e][1,2,4]thiadiazine 1,1-dioxide (5i)

EI-MS: $C_{11}H_{16}N_2O_2S$, m/z (%) =240.1 (6%) [M+].

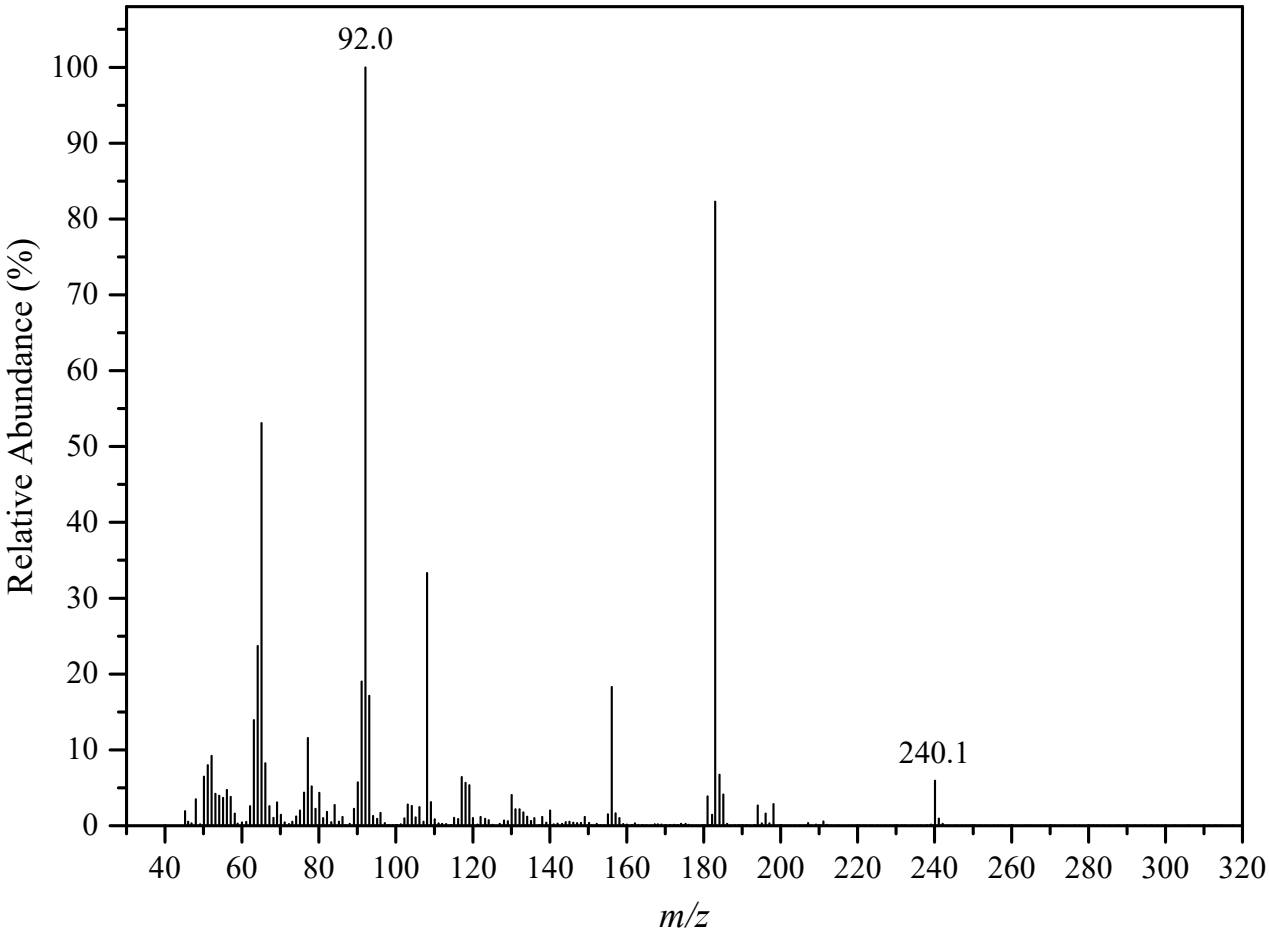

5. Notes and References

(1) Bruker, A. *APEX3* Package, *APEX3*, *SAINT* and *SADABS*. **2016**.

(2) (a) Spek, A. L. Single-Crystal Structure Validation with the Program *PLATON*. *J. Appl. Crystal.* **2003**, *36*, 7-13; (b) Spek, A. L. Structure Validation in Chemical Crystallography. *Acta Crystal.* **2009**, *D65*, 148-155; (c) Spek, A. L. What Makes a Crystal Structure Report Valid? *Inorg. Chim. Acta* **2018**, *470*, 232-237; (d) Dolomanov, O. V.; Bourhis, L. J.; Gildea, R. J.; Howard, J. A.; Puschmann, H. *OLEX2*: A Complete Structure Solution, Refinement and Analysis Program. *J. Appl. Crystal.* **2009**, *42*, 339-341; (e) Sheldrick, G. M. SHELXT–Integrated Space-Group and Crystal-Structure Determination. *Acta Crystal.* **2015**, *A71*, 3-8; (f) Sheldrick, G. M. Crystal Structure Refinement with *SHELXL*. *Acta Crystal.* **2015**, *C71*, 3-8.

(3) (a) Brese, N.; O'keeffe, M. Bond-Valence Parameters for Solids. *Acta Crystal.* **1991**, *B47*, 192-197; (b) Brown, I.; Altermatt, D. Bond-Valence Parameters Obtained from a Systematic Analysis of the Inorganic Crystal Structure Database. *Acta Crystal.* **1985**, *B41*, 244-247.

(4) Velusamy, J.; Gopal, C. S.; Kesavan, M.; Ajithkumar, A.; Swaminathan S. Construction of Indium(III)-Organic Framework Based on a Flexible Cyclotriphosphazene-Derived Hexacarboxylate as a Reusable Green Catalyst for the Synthesis of Bioactive Aza-Heterocycles. *Inorg. Chem.* **2024**, 63, 5446-5463.

(5) Liu, Y.; Zhao, P.; Duan, C.; He, C. Three-Dimensional Neodymium Metal-Organic Framework for Catalyzing the Cyanosilylation of Aldehyde and the Synthesis of 2,3-Dihydroquinazolin-4(1*H*)-one Derivatives. *Inorg. Chem.* **2023**, 62, 10359-10368.

(6) Tamoradi, T.; Mousavi, S. M.; Mohammadi, M. Praseodymium(Iii) Anchored on $CoFe_2O_4$ MNPs: An Efficient Heterogeneous Magnetic Nanocatalyst for One-Pot, Multi-Component Domino Synthesis of Polyhydroquinoline and 2,3-Dihydroquinazolin-4(1*H*)-one Derivatives. *New J. Chem*. **2020**, 44, 3012-3020.

(7) Xia, Q. C.; Zhang, S. Z.; Zhang, Y. X.; Bai, R. X.; Li, S. J.; Zhang, J.; Chen X. N. Few-Layered Metal-Organic Framework Nanosheets as Catalysts for the Synthesis of 2,3-Dihydroquinazolinone and Propargylamines. *ACS Appl. Nano Mater*. **2021**, 4, 12108-12118.

(8) Li, K.; Liu, Y. F.; Yang, G. P.; Zheng, Z. J.; Lin, X. L.; Zhang, Z. B.; Li, S. J.; Liu, Y. H.; Wei Y. G. Highly-stable Silverton-type U^{IV}-containing Polyoxomolybdate Frameworks for the Heterogeneous Catalytic Synthesis of Quinazolinones. *Green Chem*. **2024**, 26, 6454-6460.

(9) Someshwar, D. D.; Kwon, T. L.; Byung, K. C.; Yeon, T. J. Green Approach toward One Pot Cascade Synthesis of 3-Aryl-3,4-Dihydro-1,2,4-Benzothiadiazine-1,1-Dioxides. *Phosphorus, Sulfur Silicon Relat. Elem.* **2014**, 189, 40-51.

(10) Kumar, S. K.; Rambabu, D.; Kumar, C. H. V.; Sreenivas, B. Y.; Prasad, K. R. S.; Rao, M. V. B.; Pal, M. Catalysis by Amberlyst-15 under Ultrasound in Water: A Green Synthesis of 1,2,4-Benzothiadiazine-1,1-Dioxides and Their Spiro Derivatives. *RSC Adv.* **2013**, 3, 24863-24867.

(11) Du, P.; Zhou, H.; Sui, Y.; Liu, Q.; Zou, K. Asymmetric Synthesis of 3,4-Dihydro-2H-1,2,4-Benzothiadiazine-1,1-Dioxides Catalyzed by Scandium(III)-Inda-Pybox. *Tetrahedron*. **2016**, 72, 1573-1578.